MASTERARBEIT | MASTER'S THESIS

Titel | Title

Validity of kinematic analysis of Opencap in the loaded barbell squat

verfasst von | submitted by

Jonas Dandorfer B.Sc.

angestrebter akademischer Grad | in partial fulfilment of the requirements for the degree of

Master of Science (MSc)

Wien | Vienna, 2026

Studienkennzahl lt. Studienblatt | Degree programme code as it appears on the student record sheet:	UA 066 826
Studienrichtung lt. Studienblatt | Degree programme as it appears on the student record sheet:	Masterstudium Sportwissenschaft
Betreut von | Supervisor:	Univ.-Prof. Dipl.-Ing. Dr. Arnold Baca
Mitbetreut von | Co-Supervisor:	Dr. Juliana Exel Santana B.Sc. MSc.

Abstract

Markerless motion capture systems are emerging as low-cost alternatives to gold-standard infrared systems; however, their accuracy for estimating human movement kinematics must be established before widespread application in sports science. This study evaluated the accuracy of OpenCap, an open-source markerless motion capture system, compared with a marker-based reference system during the loaded barbell squat. Twenty-one participants performed three single-repetition squats at 60% and 70% of their one-repetition maximum. Agreement between systems was assessed using root mean square error (RMSE), peak error, and Bland–Altman analysis across lower-limb and pelvis kinematics. The overall RMSE across all kinematic variables was 5.58° ± 0.75° at 60% 1RM and 5.61° ± 0.90° at 70% 1RM, with mean peak errors of 10.44° ± 5.28° and 10.43° ± 5.30°, respectively. Bland–Altman analysis revealed small mean biases (~1.7–1.9°) but wide limits of agreement that exceeded a predefined acceptable threshold of ±5°, indicating limited interchangeability between systems. The largest errors were observed for pelvis motion and sagittal-plane hip and ankle kinematics. These findings indicate moderate agreement between OpenCap and the marker-based system during loaded squats. While markerless motion capture shows strong potential for biomechanical analysis, further improvements are required before it can replace gold-standard systems in high-precision sports science applications.

Zusammenfassung

Markerlose Bewegungsanalysesysteme entwickeln sich zu kostengünstigen Alternativen zu den als Goldstandard geltenden Infrarotsystemen. Allerdings muss ihre Genauigkeit bei der Schätzung der Bewegungskinematik des Menschen erst noch nachgewiesen werden, bevor sie in der Sportwissenschaft breite Anwendung finden können. In dieser Studie wurde die Genauigkeit von OpenCap, einem markerlosen Open-Source-Bewegungsanalysesystem, im Vergleich zu einem markierungsbasierten Referenzsystem bei den Kniebeugen mit Langhantel bewertet. Einundzwanzig Teilnehmer führten drei Kniebeugen mit einer Wiederholung bei 60 % und 70 % ihres Maximums durch. Die Übereinstimmung zwischen den Systemen wurde anhand des quadratischen Mittelwertfehlers (RMSE), des Spitzenfehlers sowie der Bland-Altman-Analyse für die Kinematik der unteren Extremitäten und des Beckens bewertet. Der Gesamt-RMSE über alle kinematischen Variablen betrug 5,58° ± 0,75° bei 60 % 1RM und 5,61° ± 0,90° bei 70 % 1RM, mit mittleren Spitzenfehlern von 10,44° ± 5,28° bzw. 10,43° ± 5,30°. Die Bland-Altman-Analyse ergab geringe mittlere Verzerrungen (~1,7–1,9°), jedoch breite Übereinstimmungsgrenzen, die einen vordefinierten akzeptablen Schwellenwert von ±5° überschritten, was auf eine begrenzte Austauschbarkeit zwischen den Systemen hindeutet. Die größten Fehler wurden bei der Beckenbewegung sowie bei der Kinematik der Hüfte und des Sprunggelenks in der Sagittalebene beobachtet. Diese Ergebnisse deuten auf eine moderate Übereinstimmung zwischen OpenCap und dem markerbasierten System bei Kniebeugen unter Belastung hin. Obwohl die markerlose Bewegungserfassung ein großes Potenzial für die biomechanische Analyse aufweist, sind weitere Verbesserungen erforderlich, bevor sie die Goldstandard-Systeme in hochpräzisen sportwissenschaftlichen Anwendungen ersetzen kann.

Table of Contents

Acknowledgments

First, I would like to thank my supervisors, Univ. – Prof. Dipl-Ing. Dr. Arnold Baca and Dr. Juliana Excel for their support and advice throughout the Thesis Project, as well as for making the data collection possible during my internship in the Department of Biomechanics, Kinesiology and Computer Science in Sport. I would like to thank Leon Lobe, B.Sc, for the help throughout the development process and the piloting of the research project. Furthermore, I would like to thank Dr. Willi Koller and Dr. Basilio Goncalves for the support and advice in the post-processing of the collected data.

1. Introduction

Motion capture (MoCap) technology is a core element of biomechanical analysis in sports science, providing insights into human movement kinematics (Suo et al., 2024; Wei et al., 2025). In biomechanics, optimizing athletic technique and performance while minimizing injury risk is a central objective, for which MoCap systems are commonly employed to quantify kinematic and kinetic characteristics of movement (Tai et al., 2023; Teferi & Endalew, 2020; Giustino & Patti, 2025; Adlou et al., 2025). The current gold standard for measuring kinematics is infrared marker-based systems, which provide high accuracy of up to 0.15 mm for static and 2 mm for dynamic measurements (Adlou et al., 2025). Despite their precision, these systems are associated with several practical limitations, including high cost, the requirement for specialised personnel, time-consuming setup, laboratory-bound application, and potential inaccuracies arising from skin-mounted markers, such as soft tissue artefacts or alterations of natural movement patterns (Adlou et al., 2025; Armitano-Lago et al., 2022; Horsak et al., 2023). Addressing some of these limitations, markerless MoCap systems emerged, driven by recent advances in computer vision and deep learning (Uhlrich et al., 2022). Markerless systems offer a low-cost, portable, and easy-to-use alternative that reduces preparation time and allows scientists and coaches to perform quantitative analysis of human movement kinematics in diverse environments (Armitano-Lago et al., 2022; Horsak et al., 2023; Wei et al., 2025).

Despite these advantages, markerless systems encounter challenges in sport science, primarily due to the complexity of athletic movement (Wei et al., 2025; Armitano-Lago et al., 2022). Sport-specific tasks commonly feature high velocities and accelerations and often involve multi-joint movements across several anatomical planes (Souaifi et al., 2025; Wei et al., 2025; Adlou et al., 2025). While markerless systems demonstrated agreement of 3°-15° root mean square error (RMSE) in the sagittal plane during sport-related motions like jumping and cutting, their accuracy tends to decline with tasks that require movement in the frontal or transversal planes when compared to marker-based MoCap systems (Horsak et al., 2023; Lima et al., 2024; Adlou et al., 2025). Consequently, further investigation is warranted to determine whether markerless motion capture algorithms can yield biomechanical measures suitable for analyses of complex movements.

The loaded barbell squat is a frequently studied example for a fundamental yet complex movement pattern (Pallarés et al, 2020; Rojas-Jaramillo et al., 2024; Myer et al., 2014). It is considered one of the most effective exercises for enhancing athletic performance because it recruits the major muscle groups (quadriceps, glutes, hamstrings) of the lower body, requires core stabilization, and allows high-intensity loading (Escamilla et al., 2001; Myer et al., 2014; Straub et al., 2024). The squat plays a key role in strength diagnostics, training, and competition, being a principal component in Powerlifting and weightlifting. As a diagnostic tool, the loaded barbell squat is used to evaluate strength gains and provide information to structure strength training for performance athletes, while the unloaded squat is used to identify biomechanical deficits that may elevate injury risk or limit performance (Rojas-Jaramillo et al., 2024; Myer et al., 2014). In strength training, the squat is also associated with improvements in explosive actions such as sprinting or jumping (Styles et al., 2016; Loturco et al., 2022).

Given the significance and complexity of loaded barbell squats in sport science, collecting biomechanical data on this exercise in field settings using markerless MoCap systems would be advantageous for coaches and scientists. Therefore, it is necessary to evaluate the level of agreement between the gold standard marker-based systems and markerless systems.

2. Review

2.1 Infrared marker-based systems

Optical marker-based motion capture systems are widely regarded as the gold standard for human movement analysis (Ray et al., 2024; Adlou et al., 2025). These systems function by detecting light in the infrared (IR) spectrum to estimate the position of landmarks in three-dimensional space using triangulation algorithms (Adlou et al., 2025; Liao et al., 2020). Multiple synchronized cameras, each equipped with IR light-emitting diodes arranged in a ring around the lens and utilizing either passive or active markers, are employed for data capture (van der Kruk et al., 2018).

Passive markers are spherical objects coated in retro-reflective material, reflecting IR light from the cameras back to the sensors (Das et al., 2023). In contrast, active markers emit their own IR light (van der Kruk et al., 2018). Markers are attached to specific anatomical landmarks to track their movement in three-dimensional space (Das et al., 2023). Because marker tracking relies on triangulation, each marker must be visible to at least two cameras simultaneously to accurately compute its coordinates within the global reference system (Adlou et al., 2025; Ceseracciu et al., 2014). Increasing the number of cameras that detect a marker further enhances reconstruction accuracy, setting the stage for reliable measurement.

Because each camera acquires only two-dimensional (2D) images, precise calibration is essential to accurately reconstruct three-dimensional (3D) measurements (Ceseracciu et al., 2014). During dynamic calibration, both intrinsic parameters (such as focal length and lens distortion) and extrinsic parameters (including camera position and orientation) are determined. Calibration typically involves moving an object with a known marker configuration through the capture volume while it is recorded by multiple cameras (Ceseracciu et al., 2014). Triangulation of corresponding 2D marker detections across cameras enables the estimation of 3D coordinates (Das et al., 2023).

To establish the global laboratory coordinate system, a calibration object—such as the one shown in Figure 1—is placed at a predetermined position on the measurement volume floor (Ceseracciu et al., 2014; Winter, 2009). This procedure defines the orientations of the axes and the spatial scale (Winter, 2009). Inadequate calibration can result in measurement inaccuracies. Sampling rates between 50 and 250 Hz are commonly used to capture athletic movements (Adlou et al., 2025; van der Kruk et al., 2018). The marker data acquired are utilized to calculate joint centers, kinematics, and segment positions through biomechanical musculoskeletal modeling and regression equations (Kanko et al., 2021), providing comprehensive motion analysis.

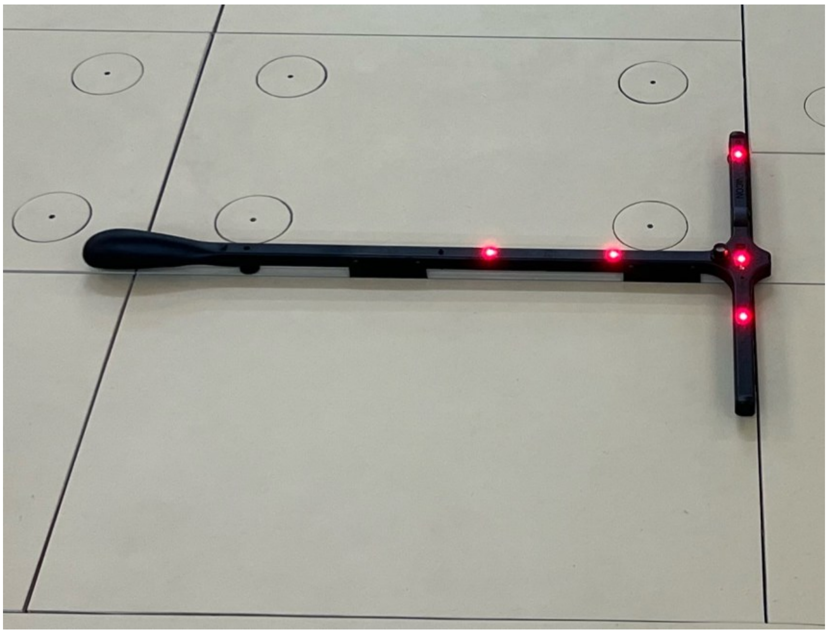

Figure 1: Calibration object used to calibrate intrinsic and extrinsic parameters, as well setting the origin for the local coordinate system

Reliability is highest in the sagittal plane, with Coefficients of Multiple Correlation (CMC) ranging from 0.89 to 0.99; slightly lower but still robust values are reported for the frontal and transverse planes (Das et al., 2023; Matsuda et al., 2025; McGinley et al., 2009). Due to this demonstrated validity and reliability, optical marker-based systems are frequently used as a reference standard when evaluating emerging technologies such as inertial measurement units or markerless motion capture systems (Adlou et al., 2025; Liao et al., 2020). This comparative role highlights their significance in the advancement of biomechanical analyses.

Despite their accuracy, marker-based systems have several constraints and limitations for movement analysis (Das et al., 2023). Because markers are affixed to the skin over anatomical landmarks, movement of the skin, muscle, or adipose tissue can produce Soft Tissue Artifacts. These artifacts may introduce errors into the estimation of the underlying skeletal movement, ranging from 3° to 11°, which exceed the system's instrumental error (Adlou et al., 2025; Das et al., 2023). These limitations necessitate careful consideration when interpreting measurement data.

In addition, attaching markers to anatomical landmarks through palpation is time-consuming, highly dependent on the operator's expertise, and requires specialized, trained personnel (Kanko et al., 2021). This operational complexity can impact the efficiency of data collection.

Moreover, infrared-based systems present several environmental and technical challenges. Bright sunlight or reflections from polished surfaces can disrupt marker detection, particularly when sport-specific equipment is used. The complexity of sports movements may also result in data gaps if limbs or equipment obstruct the camera's view of the markers (Adlou et al., 2025; Das et al., 2023). Furthermore, these systems require minimal or skin-tight clothing and the physical presence of markers, which may alter athletes' natural movement patterns and limit the ecological validity of laboratory measurements (Horsak et al., 2023; Adlou et al., 2025). The high cost and laboratory-bound nature of these setups also impose substantial financial and logistical barriers to widespread use (Horsak et al., 2023; Das et al., 2023). These constraints underscore the need for continued technological development in the field.

In summary, infrared motion capture systems represent the gold standard for human movement analysis owing to their high marker-tracking accuracy. Nevertheless, their limited portability, high cost, complex setup, and sensitivity to environmental conditions restrict widespread practical application and accessibility. Ongoing research and innovation aim to address these limitations and expand their utility in sports biomechanics.

2.2 Markerless Motion Capture systems

2.2.1 General technical background and benefits

Advancements in technology and artificial intelligence (AI) have led to the rapid emergence of markerless motion capture (MoCap) systems designed to address the constraints of marker-based systems (Mündermann et al., 2006; Armitano-Lago et al., 2022; Lam et al., 2023). Markerless systems utilize computer vision and deep learning algorithms, rather than physical sensors, to analyze human movement. Standard video cameras, recording at 25 to 240 frames per second, enable three-dimensional motion reconstruction without the need for skin-mounted reflective markers (Horsak et al., 2023; Uhlrich et al., 2023; Chaumeil et al., 2024). This technological shift forms the foundation for more accessible and flexible biomechanical analysis.

At the technological core of markerless MoCap systems are deep learning-based pose estimation algorithms (Armitano-Lago et al., 2022; Uhlrich et al., 2023). These algorithms, structured as convolutional neural networks (CNN), are trained using large datasets composed of hundreds of thousands of manually annotated images (Kanko et al., 2021; Jatesiktat et al., 2025; Wade et al., 2022). During training, networks learn to identify specific "keypoints," including joint centers and anatomical features, by analyzing pixel color, texture, and gradient patterns. To enhance biomechanical accuracy, advanced markerless systems integrate Long Short-Term Memory (LSTM) or transformer models, as standard AI models typically detect approximately 20 keypoints (Jatesiktat et al., 2025; Uhlrich et al., 2023; Falisse et al., 2025). This algorithmic complexity underpins the improved accuracy of modern motion analysis.

The elimination of physical marker placement and costly hardware in markerless MoCap allows for more cost- and time-efficient setups (Mündermann et al., 2006; Horsak et al., 2023; Scataglini et al., 2024). Marker detection of body landmarks through computer vision may reduce soft-tissue artifacts, a primary source of error in marker-based systems. Additionally, because palpation of anatomical landmarks is not required, inter-tester reliability can be improved, leading to more consistent and user-independent data analysis (Mündermann et al., 2006; Scataglini et al., 2024; Wade et al., 2022). Markerless MoCap algorithms can also estimate marker and segment locations when these are partially obscured, leveraging previously learned body geometry (Jatesiktat et al., 2025). These systems support data collection in real-world environments, thereby increasing the transferability of data due to the lack of physical markers and enhanced portability (Höltke et al., 2025; Armitano-Lago et al., 2022). Finally, the use of video-based data enables post-processing years after collection, as advancements in pose-estimation algorithms can be applied retrospectively to improve analysis (Wren et al., 2023). This progression supports the continued evolution of biomechanical research methodologies.

2.2.2 OpenCap

OpenCap is a markerless, open-source web application developed at Stanford University. It performs three-dimensional (3D) motion analysis using a minimum of two to four standard iPhone cameras (Uhlrich et al., 2023).

OpenCap's pose estimation algorithm builds upon established methods such as HRNet and OpenPose, which are trained with large-scale datasets including COCO and MPII to identify two-dimensional (2D) key points in video frames. However, these algorithms alone are insufficient for comprehensive 3D motion characterization. To address this limitation, the developers implemented a long short-term memory (LSTM) model to extrapolate a dense set of 43 anatomical markers from approximately 20 sparse video key points (Uhlrich et al., 2023; Falisse et al., 2025). The so-called "marker enhancer" was initially trained using 108 hours of motion capture data from 336 subjects, and later improved with over 1,400 hours of motion capture (MoCap) data from more than 1,000 subjects. To further enhance generalizability, the training protocol included simulated variations in subject height and multiple rotations to represent movements performed in different directions (Uhlrich et al., 2023; Falisse et al., 2025).

Calibration involves loading pre-computed intrinsic parameters, such as focal length and distortion, from a database. To determine extrinsic parameters, a printed checkerboard is positioned vertically on a flat surface. Capturing a single image enables the software to calculate the spatial relationship between the cameras and the global coordinate system (Uhlrich et al., 2023).

Because subjects do not wear physical markers, a neutral standing pose is recorded for approximately five seconds to scale a musculoskeletal model to each participant's segment lengths. The collected data are processed on a cloud server, though local processing is also possible using published GitHub scripts (Uhlrich et al., 2023). Time synchronization between mobile devices is achieved using cross-correlation of keypoint velocities across camera views. To reconstruct 3D motion, Direct Linear Transformation (DLT) is applied to project 2D points into 3D space. Subsequently, OpenCap employs inverse kinematics in OpenSim to calculate kinematic variables, such as joint angles, while respecting anatomical joint constraints (Uhlrich et al., 2023).

2.2.3 Current limitations and research gap of markerless MoCap systems

Markerless motion capture systems address many limitations inherent to marker-based systems, prompting rapid research into their validity and reliability as potential low-cost alternatives (Armitano-Lago et al., 2022). Nevertheless, the performance of markerless systems remains limited by technical and methodological constraints (Armitano-Lago et al., 2022). Notably, accuracy varies by movement plane and joint complexity, with rotational movements, pelvic kinematics, and joints with smaller ranges of motion consistently exhibiting greater errors (Scataglini et al., 2024). Systematic offsets in joint center definitions, as well as sensitivities to environmental conditions, camera configurations, and occlusions, further reduce system robustness, especially during complex and dynamic tasks (Armitano-Lago et al., 2022; Wren et al., 2023). Recent studies report that MLMC systems still face challenges in accurately capturing complex movements and subtle kinematic changes (Wren et al., 2023; Horsak et al., 2023). OpenCap, for example, shows strong validity and reliability for spatiotemporal parameters such as walking speed, stride length, and step time; however, the accuracy of kinematic data remains contingent on both the movement plane and the specific joint assessed (Lima et al., 2024; Yang, 2024; Turner et al., 2024). The greatest agreement is observed in the sagittal plane, with an RMSE of 3.3° to 5.7° for knee flexion and moderately higher RMSEs for hip flexion, ranging from 8.6° to 11.0°. In contrast, movements in the frontal or sagittal planes often exhibit higher errors for joints with a smaller range of motion. The largest RMSEs are reported in the transverse plane, with values from 6.9° to 13.2° for hip external/internal rotation (Turner et al., 2024; Horsak et al., 2023; Kanko et al., 2021).

Although the hip and knee joints exhibit moderate to good agreement in the sagittal plane, the ankle and subtalar joints present greater challenges for markerless systems. Specifically, the RMSE for ankle flexion is 11.9°, while the subtalar joint demonstrates RMSE values between 7.3° and 10.2° (Turner et al., 2024; Horsak et al., 2023).

With an average intersession error of 2.8° for walking and 3.3° for sit-to-stand tasks, OpenCap demonstrates robust reliability and eliminates human error associated with marker placement. Additionally, OpenCap is highly resilient to variations in clothing, with errors of less than 1° observed when subjects wear regular streetwear (Horsak et al., 2024).

Current research on OpenCap's validity primarily emphasizes physiological and pathological gait analysis. However, studies indicate that errors increase for tasks involving higher velocity and more complex movement patterns, such as jumping. Given that sports-related actions are characterized by high velocity and complex, multi-plane movement, further investigation into OpenCap's error rates for analyzing sports-related tasks is warranted.

2.3 The squat

The loaded barbell squat is a well-studied exercise in sports science, recognized for its beneficial effects on both performance athletes and individuals engaged in general health training, injury prevention, and rehabilitation (Schönfeld, 2010; Goodman et al., 2024). Research demonstrates a significant correlation between maximum strength and both sprint and jumping performance. Increases in overall maximum strength from the squat enhance the rate of force development, primarily through improvements in the strength–velocity relationship and neurological adaptations related to inter- and intra-muscular coordination (Hammami et al., 2019; Stone et al., 2024; Murawa et al., 2020). These adaptations contribute to greater explosive strength and power, which directly support acceleration and athletic performance in sprinting, jumping, and change-of-direction tasks.

In clinical settings, the squat and its variations are frequently employed for rehabilitation following anterior cruciate ligament (ACL) injuries and for the management of patellar tendinopathy (Stone et al., 2024; Scattone Silva et al., 2024). The squat's closed kinematic chain reduces ACL strain compared to knee extension, supporting its use for rehabilitation and lower-body strengthening (Stone et al., 2024). Additionally, the squat is widely incorporated into general health-oriented strength training. Beyond promoting hypertrophy and maximum strength in the lower body, squats improve joint stability by enhancing the structural strength and rigidity of tendons, ligaments, and cartilage. These adaptations enhance overall health and may reduce injury risk in performance athletes (Stone et al., 2024).

The squat is a multiplanar movement (Schönfeld, 2010), with most force generated in the sagittal plane by the quadriceps femoris, biceps femoris, and gluteus maximus, all of which are highly active during hip and knee flexion and extension (Van den Tillaar et al., 2024; Pürzel et al., 2025). The ankle joint, particularly its flexibility in flexion and extension, is crucial for squatting performance because it influences forward trunk inclination and the ability to maintain the center of gravity over the midfoot (Schönfeld, 2010). In the frontal plane, lateral stability and limb alignment are primarily controlled (Sohn & Koo, 2023), and both joint moments and muscle activation are strongly affected by stance width. A wider stance increases hip and knee adduction moments, as well as hip adductor activation (Larsen et al., 2021; Larsen et al., 2025). Under high-intensity loads near the one repetition maximum (1RM), knee valgus may occur (Larsen et al., 2025). In the transverse plane, ankle rotation ensures contact stability, while hip rotation is essential for maintaining joint alignment under maximum load to prevent technical failure (Sohn & Koo, 2023). The degree of hip internal rotation in the squat is also influenced by stance width (Larsen et al., 2021). Overall, the sagittal plane is key for force production, while the frontal and transverse planes primarily provide joint stabilization, underscoring the importance of multiplanar movement during the loaded barbell squat.

Kinematic analysis of the squat requires careful consideration of the lower body, particularly the knee, hip, and ankle joints, as well as the pelvis, which acts as a mechanical link between the spine and lower extremities (Schönfeld, 2010). The ankle joint forms the primary connection between the body and the ground and substantially influences both movement geometry and force production during the squat. Adequate ankle mobility is essential for maintaining balance in the deep squat; specifically, an angle of approximately 38.5° is necessary to prevent the heels from lifting off the floor (Schönfeld, 2010). When dorsiflexion is restricted and the heels lose contact, instability arises, and compensatory mechanisms increase loading on the knee, hip, and spine, thereby elevating injury risk (Schönfeld, 2010). The muscles acting on the knee joint are primary contributors to force generation in the sagittal plane, but knee movement also plays a key role in stabilizing the squat in both the frontal and transverse planes (Pürzel et al., 2025). The quadriceps femoris is the main muscle responsible for knee extension. During hip extension, hamstring activation generates a flexion moment at the knee, which the quadriceps femoris must offset (Larsen et al., 2024; Bryanton et al., 2012). Importantly, the force produced by the hamstrings reduces stress on the ACL, a critical consideration given the high compressive forces experienced by the knee joint during the squat (Pürzel et al., 2025; Schönfeld, 2010).

During the initial phase of the concentric movement, knee flexion and extension dominate force production, whereas the hip joint bears the primary load in the critical final phase (Van den Tillaar et al., 2024; Larsen et al., 2021). The literature frequently identifies hip extension as a key determinant of squat performance. In this critical phase, the hip may contribute approximately 51.5% to 54.4% of the body's total support moment. Failed repetitions often result from insufficient hip extension strength to overcome the demands at the bottom of the deep squat (Larsen et al., 2025; Larsen et al., 2021). Additionally, controlling external rotation moments is necessary to prevent knee valgus and to stabilize both the pelvis and knee joint (van den Tillaar & Larsen, 2020; Larsen et al., 2021; Schönfeld, 2010). These findings highlight the central role of the hip joint in the loaded barbell squat.

The pelvis serves as a mechanical link between the lower extremities and the spine, regulating power transmission and joint alignment (Larsen et al., 2024; van den Tillaar & Larsen, 2020). Pelvic tilt, in particular, is crucial for maintaining the stability and integrity of the lumbar spine (Schönfeld, 2010). During the barbell squat, excessive posterior tilt—commonly referred to as the "Butt Wink"—can position the spine disadvantageously, substantially increasing shear forces in the lumbar region (van den Tillaar & Larsen, 2020; Schönfeld, 2010). Thus, effective control of pelvic position is essential for spinal safety throughout the squat.

Active stabilization of the pelvis is particularly important during the free weight squat to ensure proper alignment of the tibia and femur. Instability in this region increases activation of the gluteus maximus and gluteus medius, which may reduce their ability to effectively contribute to hip extension (Larsen et al., 2021; van den Tillaar & Larsen, 2020; Schönfeld, 2010).

Recent studies report a high range of motion (ROM) during the squat. The greatest ROM occurs in the sagittal plane during knee flexion, with means ranging from 125.3° to 126.4°, and sometimes exceeding 140°. Mean hip flexion falls between 105.7° and 111.8°, while ankle flexion exceeds 30°. Maximum hip adduction in the frontal plane is 25.4°, and hip rotation in the transverse plane reaches 15.4° (Larsen et al., 2021). These findings demonstrate that the squat approaches the anatomical ROM limits of the lower body.
Furthermore, kinematic variables in the barbell squat are influenced by different loading conditions (Larsen et al., 2022; Sohn & Koo, 2023). With increasing load, literature suggests that athletes tend to lean their trunk forward to keep the center of gravity above the point of support or compensate for fatigue in the back extensors (Schönfeld, 2010). Alongside analysis reveals an increase in hip extension and a decrease in knee and ankle flexion with increasing loads (Larsen et al., 2022). This emphasizes the importance of the hip joint during the loaded squat (Larsen et al., 2021; Larsen et al., 2022). Additionally, barbell speed decreases with increasing intensity, and a more pronounced sticking region emerges, in which barbell velocity declines and the risk of failure peaks during the concentric phase of the movement (Larsen et al., 2021).

Overall, the loaded barbell squat exhibits a complex kinematic pattern across all planes of motion and confers substantial benefits for sport performance and general health.

2.4 Research question

Evidence regarding the accuracy of markerless motion-capture systems, such as OpenCap, in sport-specific tasks remains limited. Most validation studies have focused on clinical biomechanics, with an emphasis on gait and walking-based assessments. While recent research has begun to assess markerless systems during high-velocity bodyweight movements (e.g., jumping and change-of-direction tasks), there remains a lack of accuracy data for loaded strength exercises, which typically involve complex, multiplanar movement patterns. This gap highlights the need for further investigation into markerless motion capture in the context of loaded exercises.

The squat represents a biomechanically complex exercise, involving large ranges of motion and coordinated actions across all three planes. Due to its established effectiveness in enhancing sports performance and promoting general health, the squat is one of the most extensively studied resistance exercises. Consequently, the loaded barbell squat serves as an ecologically valid and practical task for evaluating agreement between markerless and marker-based motion-capture systems. Building on this rationale, the present study aims to determine whether the markerless system OpenCap yields joint kinematic measurements for the hip, knee, ankle, and pelvis that are comparable to those from a gold-standard marker-based system (Vicon) during the loaded barbell squat and whether the difference between the systems increases with different loading characteristics. These aims provide a foundation for further analysis of system agreement in this context.

The literature indicates that a mean bias of 2° or less and a 5° range for the limits of agreement, as calculated using Bland-Altman analysis, represent good agreement between systems in clinical practice (Bland & Altman, 1999). In the current literature, an RMSE in joint kinematics between 2° and 5° is considered acceptable for biomechanical clinical practice (Horsak et al., 2023; Kanko et al., 2021). Based on these standards, it is hypothesized that the markerless system will demonstrate a mean bias under 2°, a limit of agreement within 5°, and an RMSE not exceeding 5°, thereby indicating good agreement with the marker-based MoCap system.

3. Methods

3.1 Participants

This study recruited twenty-one healthy participants (11 male, 10 female) with a mean age of 23.7 ± 2.8 years, body mass of 71.6 ± 10.4 kg, and height of 174.0 ± 9.8. To be included in the study, participants had to be 18 years old, free from current or recent (within 4 weeks) lower-body injuries, and have experience performing the barbell squat at least once a week. to ensure the safety of performing a deep barbell squat. Six volunteers were active powerlifters. For these individuals, the maximal load achieved during competition within the previous 4 weeks could be used as their 1RM, provided a test leader was present at the University Championships in Vienna to verify the squat's intensity and depth. The mean 1RM for the squat in this population was 103,5 kg ± 40. The study was approved by the ethics committee of the University of Vienna (Protocol number: 01252), and all participants provided written informed consent. Based on previously reported standard deviations of the RMSE for joint kinematics (1.5°–2.7°) across functional tasks (Uhlrich et al., 2022), a medium effect size (Cohen's d = 0.74) was assumed for this analysis.An a priori power analysis (G*Power, α = 0.05, power = 0.80) indicated a minimum sample size of 17 participants for a paired-samples design, which was exceeded in the current study, thereby ensuring adequate statistical power.

3.2 Experimental Design

The experimental design required data collection over two separate days for each participant. On the first day, participants received detailed information about the study procedures, and their one-repetition maximum (1RM) in the deep barbell squat was assessed. The second day was dedicated to biomechanical testing, conducted in the biomechanics laboratory of the Institute for Sports Science at the University of Vienna. To minimize fatigue effects, at least 48 hours elapsed between testing sessions. Participants were also instructed to refrain from intensive exercise for 24 hours before each test day. Six volunteers were active powerlifters. For these individuals, the maximal load achieved during competition within the previous 4 weeks could be used as their 1RM, provided a test leader was present at the University Championships in Vienna to verify the squat's intensity and depth.

3.2.1 1RM – Test

Assessment of the 1RM squat was performed to determine individualized loads for the biomechanical analysis. Testing took place in the strength laboratory within the Department of Training Science at the University of Vienna. Before beginning the 1RM test, participants estimated their 1RM. This estimate guided a standardized warm-up protocol, which involved incremental increases in load from 50% to 90% of the estimated 1RM in 10% steps, with 4–5-minute rest intervals between sets. The protocol allowed for a maximum of five trials, with volume decreasing as intensity increased. Participants completed a self-selected warm-up routine—such as cycling on an ergometer and performing mobility exercises—prior to the main protocol. After warming up, participants attempted their first 1RM lift using their estimated 1RM as the starting load. If this load was insufficient, it was increased by a minimum of 2.5 kg. In the event of a failed attempt, the participant could either reattempt once or the load could be reduced. A 4–5-minute rest was provided between attempts, and the final 1RM had to be achieved within five attempts to limit fatigue. This systematic approach ensured reliable determination of 1RM values, supporting subsequent motion capture analysis.

3.2.2 Motion Capture analysis

During biomechanical testing, all participants were instructed to perform six single-repetition squats—three at 60% 1RM and three at 70% 1RM—while both marker-based and markerless motion capture data were collected simultaneously. Experienced strength-training spotters were present throughout to ensure participant and equipment safety. After unracking the barbell, participants moved approximately 2 meters from the squat rack to assume the starting position. For marker-based motion capture, a 13-camera system (Nexus 2.16, Vicon, Oxford, UK) recorded 42 skin-mounted markers at 200 Hz using the PyCGM 2.5 markerset (Lebeoeuf et al., 2019), with four additional markers on the pelvis and no markers on the upper limbs or head (Fig. 2). A static T-pose was recorded for each participant before dynamic data collection. This dual recording setup provided comprehensive data for subsequent analysis using both capture modalities.

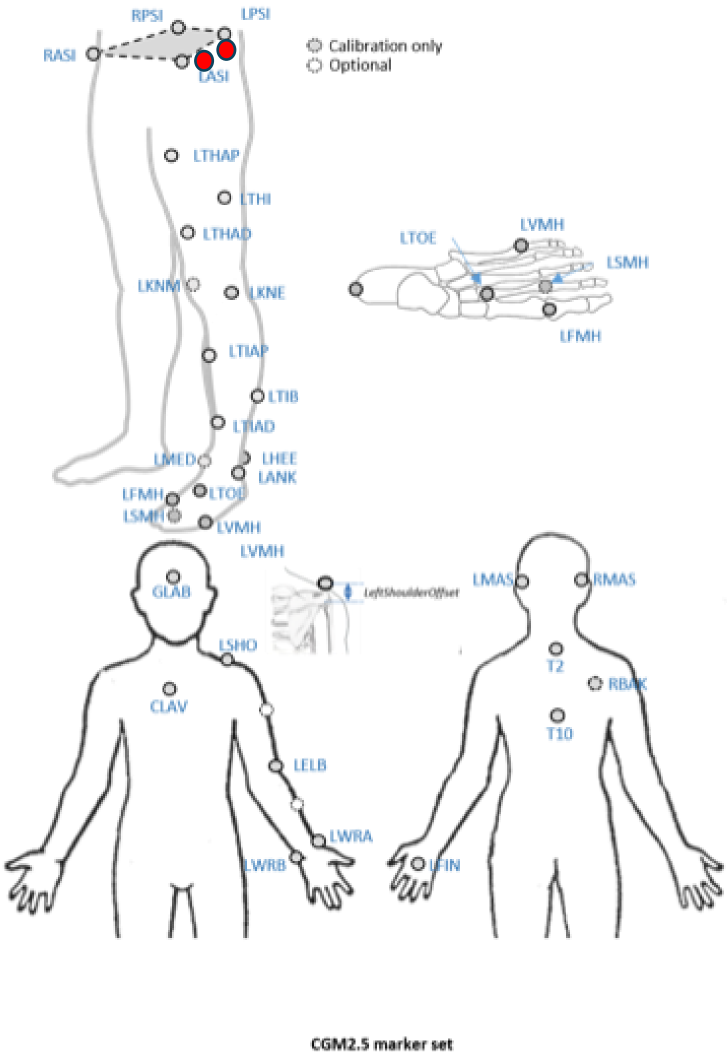

Figure 2*: PyCGM 2.5 Markerset with additional pelvis markers (red). The Markerset used in this study did not include the upper extremities or the head. (https://pycgm2.netlify.app/cgm/cgm2.5/)*

Markerless motion capture (MoCap) data were collected using the OpenCap web application and three iOS smartphones (iPhone SE, 3rd generation), following OpenCap's best-practice recommendations. Smartphones were mounted on tripods at a height of 1.1 m and positioned 3 m from the markerless MoCap recording volume (Fig. 3). Video recordings were made at a resolution of 720 × 1280 pixels and a frame rate of 120 Hz, with the pose estimation algorithm set to OpenPose in the advanced settings. As with the marker-based system, participants performed a static T-pose before dynamic data collection commenced. This procedure ensured consistency between capture methods for subsequent comparative analysis.

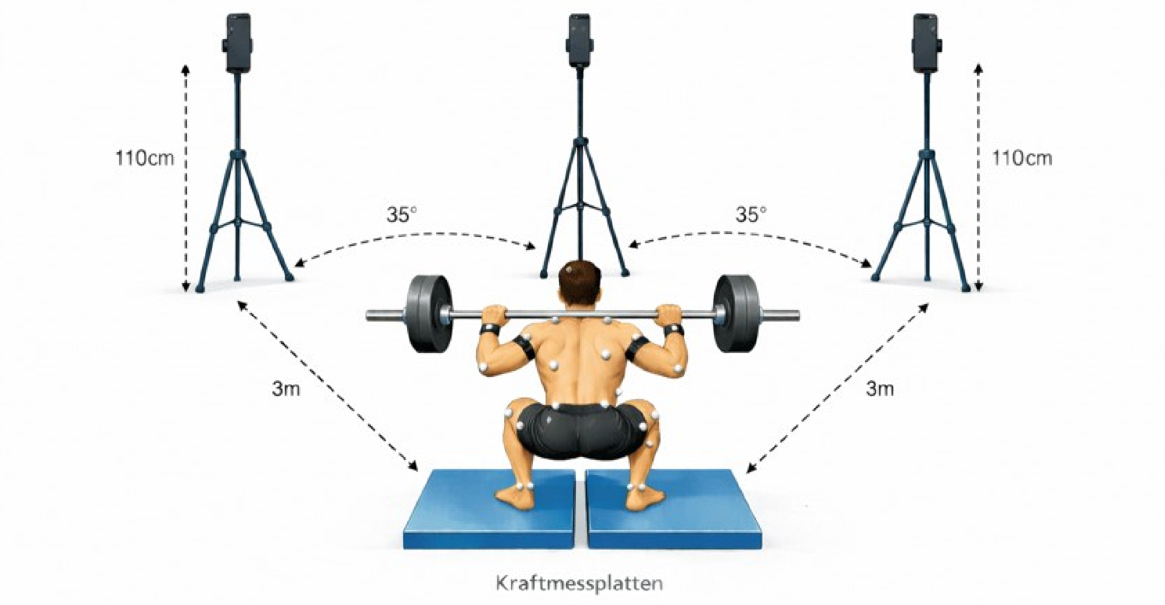

Figure 3: *Setup for markerless MoCap. Three iPhones were placed 3m away from the area of interest, while two cameras were spread out in a 35° angle. The smartphones were mounted on tripods at a height of 110 cm. Participants performed the squats on two force plates. The marker set shown in this figure is not the original marker set used in the study, but rather a fictional markerset. (Figure was created with the help of AI)*

3.3 Data analysis

3.3.1 Kinematic analysis

Marker-based data were processed using OpenSim's scaling and inverse kinematics tools, with the LaiUhlrich 2022 model applied to facilitate comparison between marker-based and markerless MoCap systems. This model is based on the musculoskeletal frameworks of Lai et al. (2017) and Rajagopal et al. (2016), incorporating modified hip abductor muscle paths (Delp et al., 2007; Uhlrich et al., 2023).

Markerless data were processed using the OpenCap web application, which also implements the LaiUhlrich 2022 model (Uhlrich et al., 2023). The version of OpenCap utilized in this study spanned from March 2025 to June 2025.

3.3.2 Statistical analysis

Statistical analyses were conducted using Python version 3.11.14. The squat cycle was identified by tracking the vertical displacement of the pelvis segment (pelvis_ty). The start of the squat was defined as the earliest point at which the pelvis exhibited a sustained downward displacement of at least 1% of the movement amplitude within a 40-frame window, marking the onset of the eccentric phase. The end of the squat was defined as the point when the pelvis returned to within 4% of the movement amplitude relative to the standing position, indicating completion of the concentric phase. The interval between these two events was extracted and defined as the squat cycle for kinematic analysis. From the initial data, 29 trials needed to be excluded for pelvis rotation and 9 for pelvis tilt due to technical problems with either the markerless or the marker-based system, resulting in a pelvis segment displacement that could not be corrected during data processing. This yields a total of N = 126 trials for the variables knee-angle, ankle-angle, subtalar-angle, hip-flexion, hip-adduction, hip-rotation, and pelvis-list. For pelvis rotation, 101 trials were included, and for pelvis tilt, 117 trials.

Agreement between the markerless and marker-based reference systems was evaluated using RMSE, peak error, and Bland–Altman analysis, computed for both loading conditions and each kinematic variable.

The root mean square error (RMSE) was used to quantify the overall magnitude of disagreement between the two systems across the entire movement cycle. For each participant, trial, joint kinematic variable, and condition, RMSE was calculated as follows:

$$RMSE = \sqrt{\left(\left(\frac{1}{N}\right)\sum_{i=1,\ldots,N}\left(x_i^{OpenCap} - x_i^{Vicon}\right)^2\right)}$$

Where x_{OpenCap}, i and x_{Vicon}, i denote the joint angles obtained from OpenCap and the marker-based system at the i-th time point of the squat cycle, and N=101 represents the number of time-normalized samples.

This computation yielded a single RMSE per trial, reflecting the average absolute difference between the two systems across the full squat cycle. RMSE values were then averaged across trials and participants to obtain condition-specific and variable-specific mean RMSE values. In addition, an overall RMSE was calculated by averaging RMSE values across all joint kinematic variables.

To complement RMSE and capture potential extreme deviations between systems, peak error was calculated as the maximum absolute difference between OpenCap and the marker-based system observed at any time point during the squat cycle:

$$Peak\ Error = \max_{i=1,\ldots,N}\left|x_i^{OpenCap} - x_i^{Vicon}\right|$$

Peak error, therefore, represents the largest instantaneous discrepancy between the two systems within a trial. As with RMSE, peak error values were computed at the trial level and then averaged across trials and participants for each joint kinematic variable and loading condition.

Bland–Altman analysis was performed to calculate the mean difference (bias) for each joint kinematic variable and to determine the corresponding 95% limits of agreement. Differences were computed across the time-normalized movement cycle and pooled across trials and participants. The limits of agreement were defined as the bias ± 1.96 times the standard deviation of the differences (Bland & Altman, 1999). Proportional bias was assessed using linear regression of the differences against the mean values, while heteroscedasticity was evaluated by correlating the absolute differences with the corresponding means. The agreement was assessed against a predefined acceptable difference of ±5°.

Statistical Parametric Mapping (SPM) was used to identify condition-dependent differences in lower-limb joint kinematics between the 60% and 70% loading conditions. Joint angle waveforms were averaged at the trial level and across left and right sides where applicable, and time-normalized to 100% of the squat cycle. Paired SPM t-tests were conducted for each kinematic variable using the SPM1D package (v0.4.18; Pataky, 2012). Normality of the residuals was assessed using the SPM1D implemented normality test and was satisfied for all variables. Statistical inference was performed using random field theory with an alpha level of .05 to control the family-wise error rate. Significant supra-threshold clusters were identified, and cluster-level p-values were reported. All SPM analyses were based on data from 21 participants (df = 1, 20).

To evaluate whether kinematic differences identified by SPM were reflected in the agreement between measurement systems, Root Mean Square Error (RMSE) and mean bias were calculated for each joint kinematic variable and loading condition. Changes in kinematic movement patterns could result in different error values, since changes could lead to limb occlusion impairing the landmark tracking. Subject-level RMSE and mean bias values were obtained by averaging across trials within each condition. Paired comparisons between the 60% and 70% conditions were performed separately for RMSE and mean bias. Normality of paired differences was assessed using the Shapiro–Wilk test; paired t-tests were applied when normality was met, and Wilcoxon signed-rank tests otherwise. Effect sizes were reported as Cohen's *d* for parametric tests and rank-biserial correlation (*r*) for nonparametric tests. Statistical significance was set at $p < .05$.

4. Results

4.1 Load-dependent differences in kinematic values, RMSE, and mean bias

Statistical Parametric Mapping (SPM) analysis was conducted to compare lower-limb joint kinematics between the 60% and 70% loading conditions using paired t-tests across the full squat cycle for the markerless and the marker-based system. Significant condition-dependent differences were identified for hip flexion, hip adduction, and knee flexion for the marker-based system. Hip flexion showed two distinct significant clusters, occurring at 31.2–36.3 % of the squat cycle (p = .032) and 65.2–79.5 % (p = .0015). Hip adduction exhibited one significant cluster between 65.2–75.1 % of the squat cycle (p = .0146). Knee flexion demonstrated one large significant cluster spanning 60.5–83.0 **%** of the squat cycle (p < .001). No significant differences were observed for pelvis tilt, pelvis list, pelvis rotation, hip rotation, ankle flexion, or subtalar angle (all p > .05). For the markerless system the SPM analysis revealed significant condition-dependent differences in the hip flexion, knee flexion, hip adduction, and the subtalar angle. Hip flexion showed one distinct significant cluster, occurring at 60.0–81.5% (p < 0.001). Hip adduction exhibited one significant cluster between 67.9–76.1 % of the squat cycle (p = .0115). Knee flexion demonstrated one large significant cluster spanning 60.4–84.7 % of the squat cycle (p < .001). The subtalar angle demonstrates one small significant cluster between 36.4 - 44.0% of the squat cycle (p = 0.0042). No significant differences were observed for pelvis tilt, pelvis list, pelvis rotation, hip rotation, ankle flexion, or subtalar angle (all p > .05). All analyses were based on 21 participants (degrees of freedom = 1, 20). Critical thresholds ($t*$) were determined using random field theory to control the family-wise error rate.

To evaluate whether these kinematic differences were reflected in the agreement between the markerless and the marker-based reference system, paired t-tests were conducted on RMSE and mean bias values for each variable. For hip flexion, the RMSE did not differ significantly between conditions (60%: M = 8.31°; 70%: M = 8.69°), t (20) = 1.45, p = .163, d = 0.32. In contrast, the mean bias differed significantly, with a more negative bias at 70% (60%: M = −3.33°, 70%: M = −4.31°), t (20) = −2.72, p = .013, d = −0.59. For knee flexion, no significant differences were found for either RMSE (60%: M = 4.78°, 70%: M = 4.74°), t (20) = −0.21, p = .833, d = −0.05, or mean bias (60%: M = 1.31°, 70%: M = 0.73°), t (20) = −2.07, p = .051, d = −0.45, although the latter showed a trend toward significance.

Similarly, hip adduction showed no significant differences between conditions for RMSE (60%: $M = 1.99°$, 70%: $M = 2.03°$), $t\,(20) = 0.66$, $p = .516$, $d = 0.14$, or mean bias (60%: $M = 1.47°$, 70%: $M = 1.59°$), $t\,(20) = 1.80$, $p = .088$, $d = 0.39$.

The corresponding boxplots (Fig. 4) illustrate the distribution of RMSE and mean bias values for hip flexion, knee flexion, and hip adduction across both loading conditions. Across all variables, a high degree of within-condition variability was observed, reflected by wide interquartile ranges and substantial overlap between the 60% and 70% conditions. Individual subject trajectories revealed pronounced inter-individual differences, with changes between conditions varying considerably in both magnitude and direction. For knee flexion and hip adduction, the distributions of RMSE and mean bias largely overlapped between conditions, indicating no clear differences at the group mean level. In contrast, hip flexion showed a shift toward a more negative mean bias at 70%, while RMSE values remained comparable between conditions. However, this shift was accompanied by substantial dispersion of individual data points, such that the large variability within each condition limited clear separation between the two loading levels. Overall, the boxplots demonstrate that although group mean differences in RMSE and mean bias between the 60% and 70% conditions were small or absent for most variables, the pronounced variability within conditions and large inter-individual differences reduced the ability to distinguish condition-dependent changes in agreement metrics.

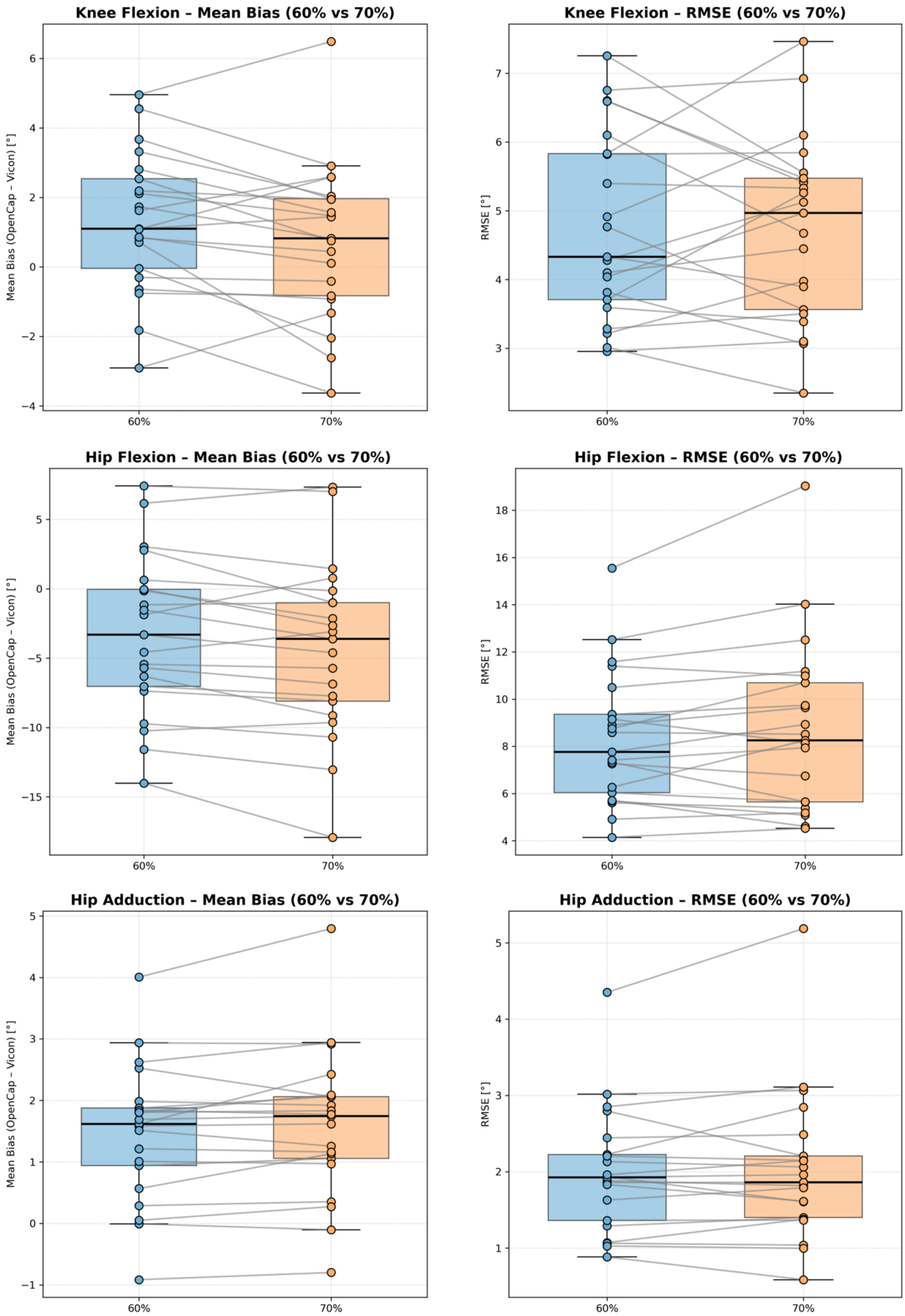

Figure 4: *Boxplots evaluating the differences in the RMSE and mean Bias of the knee flexion, hip flexion, and hip adduction between both loading conditions, 60% and 70% of 1RM in the deep barbell squat.*

4.2 *Agreement between the marker-based and the markerless system*

To evaluate agreement between the marker-based and markerless systems, Bland-Altman analysis, RMSE, and peak errors were calculated for each loading condition. Bland–Altman analysis showed a mean bias (mean difference) of 1.89° ± 6.61 ° for the 60%1RM condition. The 95% limits of agreement (LoA) ranged from −11.07° to 14.84° (95% CI for the lower LoA: −11.14°; 95% CI for the upper LoA: 14.91°). Inspection of the Bland–Altman plot revealed no relevant evidence of proportional bias (slope = −0.03, p = .04) or heteroscedasticity (r = .00, p = 1.00). Compared with the predefined acceptable difference of ±5°, the LoA exceeded the acceptable range, indicating that the two measurement systems cannot be considered interchangeable. For the 70%1RM condition, Bland–Altman analysis showed a mean bias (mean difference) of 1.71° ± 6.66°. The 95% limits of agreement (LoA) ranged from −11.35° to 14.78° (95% CI for the lower LoA: −11.42°; 95% CI for the upper LoA: 14.85°). Inspection of the Bland–Altman plot revealed no relevant evidence of proportional bias (slope = −0.04, p < .001) or heteroscedasticity (r = .06, p < .001). Compared with the predefined acceptable difference of ±5°, the LoA exceeded the acceptable range, indicating that the two measurement systems cannot be considered interchangeable. Joint and plane-specific details are provided in tables 1,3 and 5, as well as visually presented in figures 5-8.

The analysis of the mean overall RMSE across all kinematic variables revealed an error of 5.58° ± 0.75° for the 60% 1RM condition and 5.61° ± 0.90° for the 70% 1RM condition (N = 21 for both conditions). The mean peak error across all kinematic variables was 10.44° ± 5.28° for the 60% 1RM condition and 10.43° ± 5.3° for the 70% 1RM loading condition. Joint and plane-specific details are displayed in tables 2,4 and 6, as well as visually presented in figures 9-12.

Table 1: *Mean (SD) of Bland–Altman analysis outcomes for the agreement between the marker-based and markerless measurements of sagittal-plane lower-body kinematics during deep squats, separate for the 60% and 70% loading condition.*

Mean	Bias (°)		Lower LoA (°)		Upper LoA (°)	
Condition	60%1RM	70%1RM	60%1RM	70%1RM	60%1RM	70%1RM
Knee flexion (SD)	1,31 (5,09)	0,71 (5,15)	-8,66	-9,38	11,28	10,80
Ankle flexion (SD)	6,81 (5,67)	7,03 (4,99)	-4,30	-2,75	17,91	16,80
Hip flexion (SD)	-3,33 (8,35)	-4,23 (8,49)	-19,71	-20,86	13,04	12,40
Pelvis tilt (SD)	3,98 (8,16)	3,99 (8,33)	-12,01	-12,34	19,97	20,32

Table 2: *Mean (SD) of the RMSE and peak error outcomes for the agreement between the marker-based and markerless measurements of sagittal-plane lower-body kinematics during deep squat, separate for the 60% and 70% loading condition.*

Mean (SD)	RMSE (°)		Peak error (°)	
Condition	60% 1RM	70% 1RM	60% 1RM	70% 1RM
Knee flexion	4,78 (1,57)	4,71 (1,55)	12,36 (5,04)	12,17 (5,00)
Ankle flexion	7,95 (2,84)	7,75 (2,67)	13,54 (3,42)	13,27 (3,36)
Hip flexion	8,31 (2,97)	8,62 (3,58)	15,37 (4,18)	15,67 (5,37)
Pelvis tilt	8,36 (3,57)	8,52 (3,60)	14,17 (4,64)	14,17 (4,85)

Table 3: *Mean (SD) of Bland–Altman analysis outcomes for the agreement between the marker-based and markerless measurements of frontal-plane lower-body kinematics during deep squats, separate for the 60% and 70% loading condition.*

Mean (SD)	Bias (°)		Lower LoA (°)		Upper LoA (°)	
Condition	60%1RM	70%1RM	60%1RM	70%1RM	60%1RM	70%1RM
Hip adduction	1,47 (3,48)	1,60 (3,40)	-5,35	-5,07	8,29	8,27
Pelvis list	0,20 (3,86)	-0,40 (3,30)	-12,01	-6,87	7,76	6,07

Table 4: *Mean (SD) of the RMSE and peak error outcomes for the agreement between the marker-based and markerless measurements of frontal-plane lower-body kinematics during deep squats, separate for the 60% and 70% loading condition.*

Mean (SD)	RMSE (°)		Peak error (°)	
Condition	60% 1RM	70% 1RM	60% 1RM	70% 1RM
Hip adduction	1,99 (0,87)	2,03 (0,99)	3,56 (1,23)	3,56 (1,53
Pelvis list	2,76 (2,73)	2,78 (1,83)	5,47 (3,95)	5,63 (3,00)

Table 5: *Mean (SD) of Bland–Altman analysis outcomes for the agreement between the marker-based and markerless measurements of transverse-plane lower-body kinematics during deep squats, separate for the 60% and 70% loading condition.*

Mean (SD)	Bias (°)		Lower LoA (°)		Upper LoA (°)	
Condition	60%1RM	70%1RM	60%1RM	70%1RM	60%1RM	70%1RM
Hip rotation	2,96 (4,11)	2,98 (3,89)	-5,09	-4,64	11,01	10,60
Pelvis rotation	-1,04 (6,91)	-1,03 (7,36)	-14,58	-15,45	12,49	13,39
Subtalar angle	3,12 (6,72)	3,33 (6,50	-10,05	-9,41	16,29	16,07

Table 6: *Mean (SD) of the RMSE and peak error outcomes for the agreement between the marker-based and markerless measurements of transverse-plane lower-body kinematics during deep squats, separate for the 60% and 70% loading condition.*

Mean (SD)	RMSE (°)		Peak error (°)	
Condition	60% 1RM	70% 1RM	60% 1RM	70% 1RM
Hip rotation	3,60 (1,30)	3,58 (1,36)	7,84 (2,31)	8,16 (2,55)
Pelvis rotation	6,56 (2,41)	6,98 (2,59)	10,38 (3.02)	10,51 (3,18)
Subtalar angle	6,25 (2,36)	6,15 (2,17)	11,28 (3,29)	11,22 (2,92)

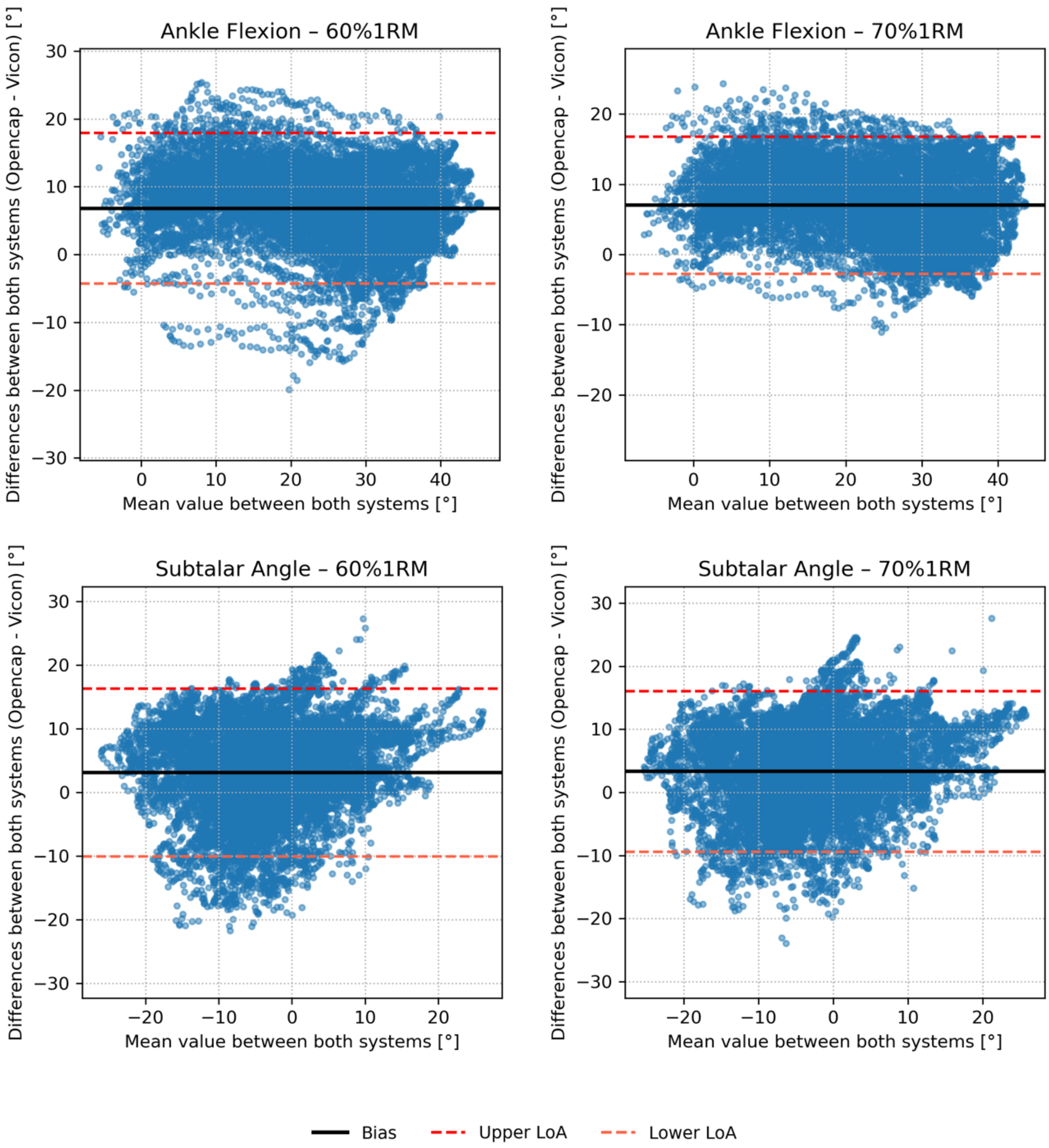

Figure 5. *Bland–Altman plots showing agreement between marker-based and markerless lower-body kinematics during deep squats in the ankle joint. The x-axis displays the mean of both measurement systems, and the y-axis represents their difference (markerless – marker-based). Solid black lines indicate mean bias, and dashed red lines indicate the limits of agreement (± 1.96). Plots are presented separately for both loading conditions.*

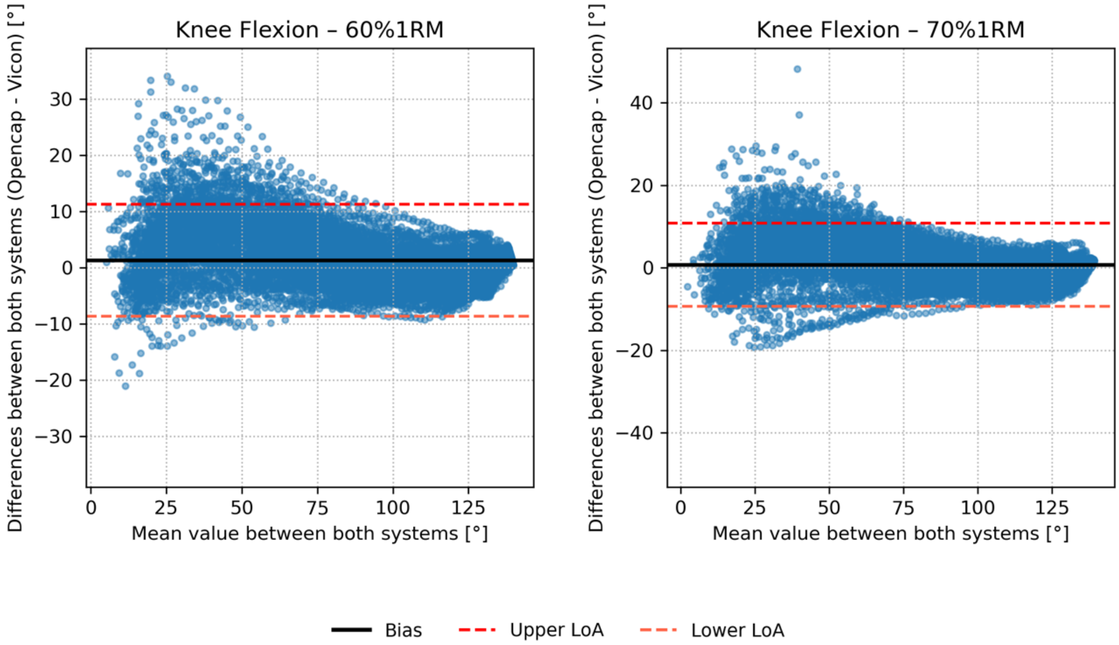

Figure 6. *Bland–Altman plots showing agreement between marker-based and markerless lower-body kinematics during deep squats in the knee joint. The x-axis displays the mean of both measurement systems, and the y-axis represents their difference (markerless – marker-based). Solid black lines indicate mean bias, and dashed red lines indicate the limits of agreement (± 1.96). Plots are presented separate for both loading conditions.*

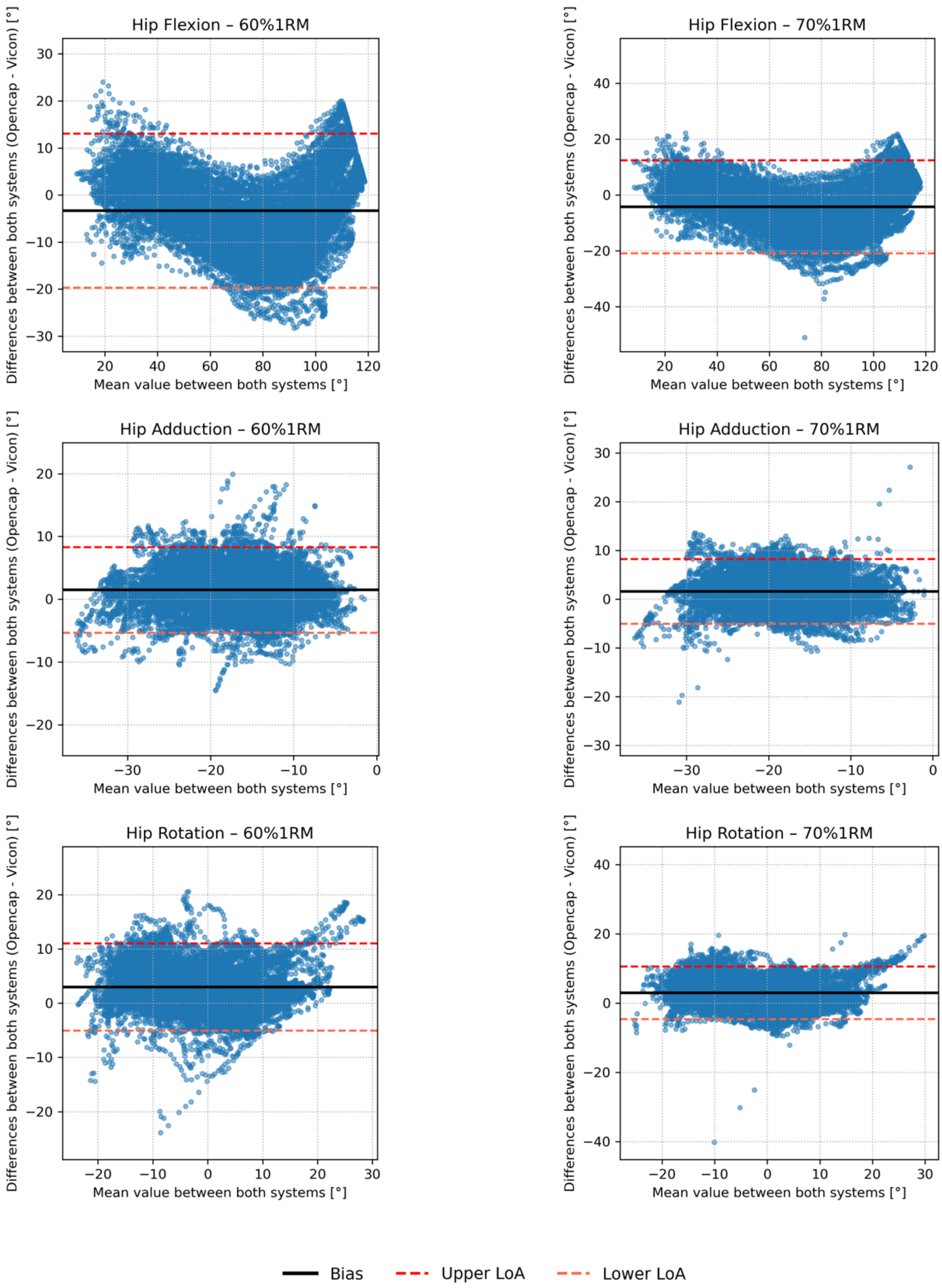

Figure 7. *Bland–Altman plots showing agreement between marker-based and markerless lower-body kinematics during deep squats in the hip joint. The x-axis displays the mean of both measurement systems, and the y-axis represents their difference (markerless – marker-based). Solid black lines indicate mean bias, and dashed red lines indicate the limits of agreement (± 1.96). Plots are presented separate for both loading conditions.*

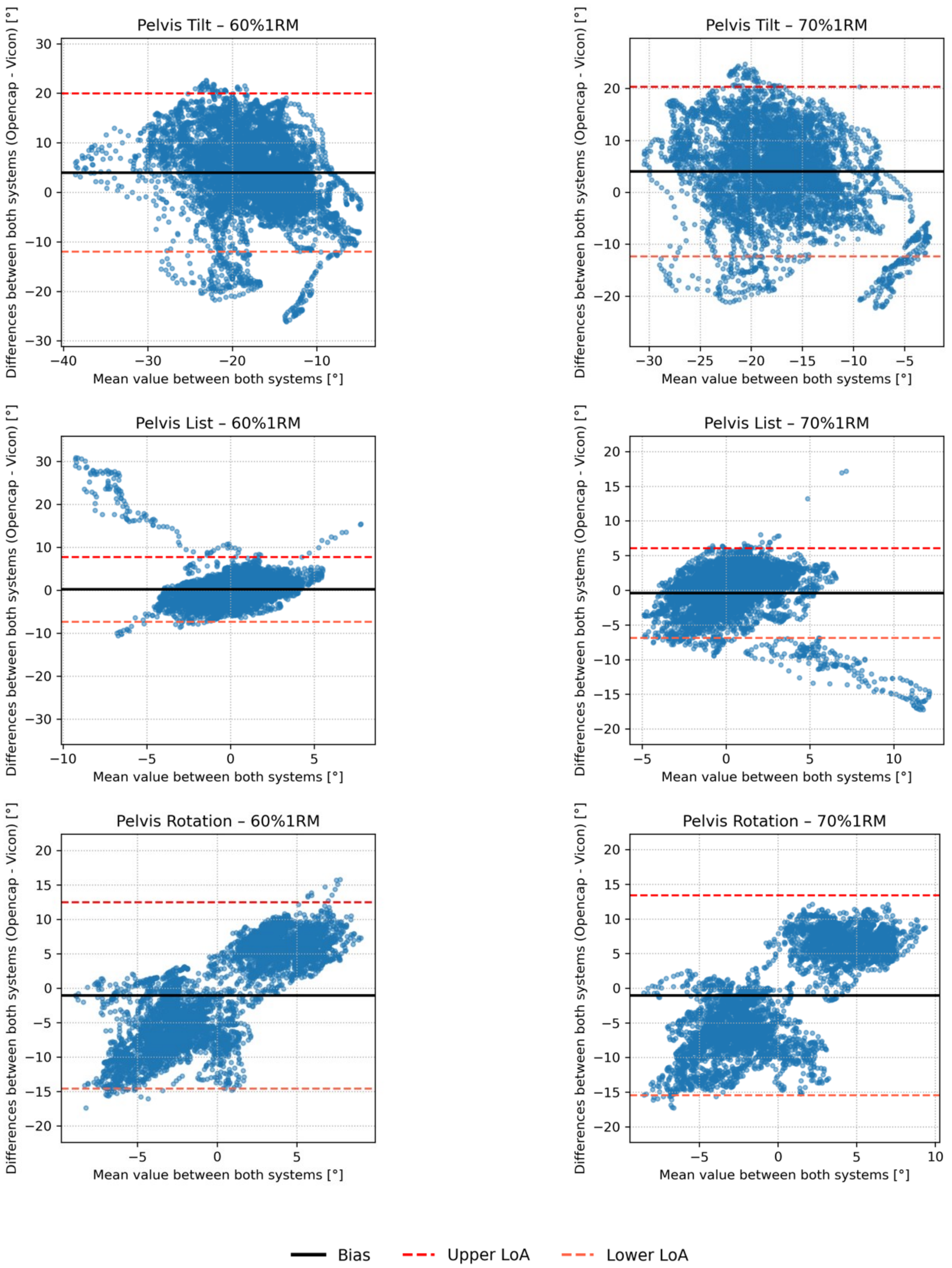

Figure 8. *Bland–Altman plots showing agreement between marker-based and markerless lower-body kinematics during deep squats in the pelvis segment. The x-axis displays the mean of both measurement systems, and the y-axis represents their difference (markerless – marker-based). Solid black lines indicate mean bias, and dashed red lines indicate the limits of agreement (± 1.96). Plots are presented separate for both loading conditions.*

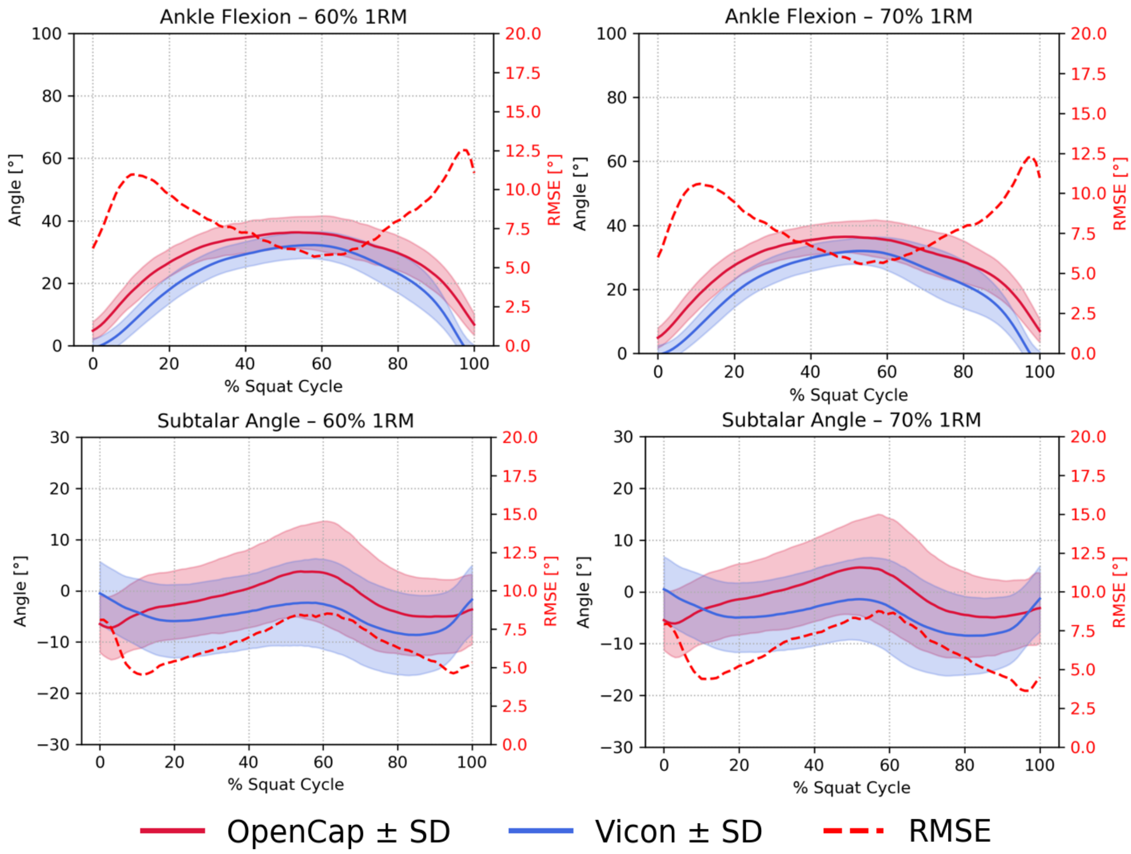

Figure 9: *Waveform-plots displaying the ankle joint kinematics for the deep squat recorded with the markerless (red) and marker-based (blue) motion capture systems. The secondary axis shows the RMSE (red dashed) calculated per frame over the waveform of the squat cycle between both systems. Plots are presented separately for both loading conditions.*

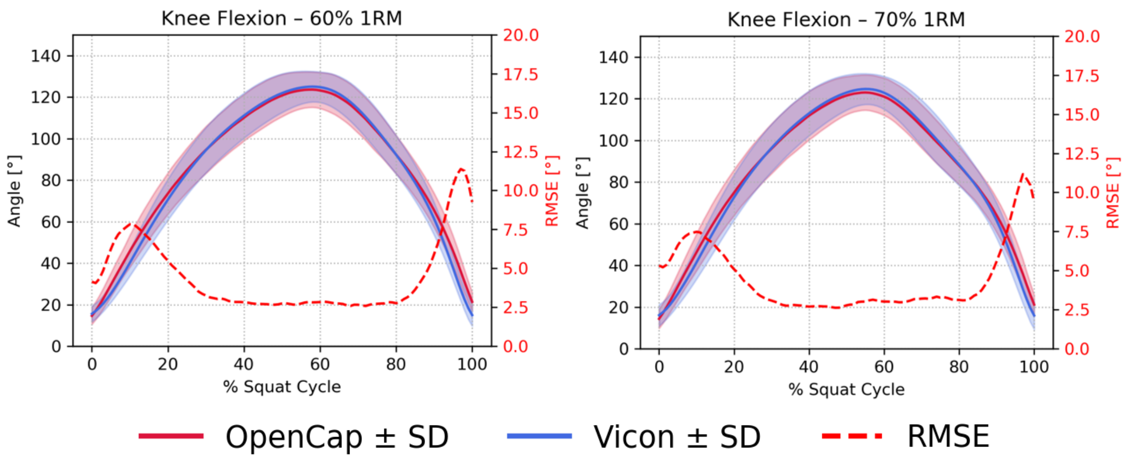

Figure 10: *Waveform-plots displaying the knee joint kinematics for the deep squat recorded with the markerless (red) and marker-based (blue) motion capture systems. The secondary axis shows the RMSE (red dashed) calculated per frame over the waveform of the squat cycle between both systems. Plots are presented separately for both loading conditions.*

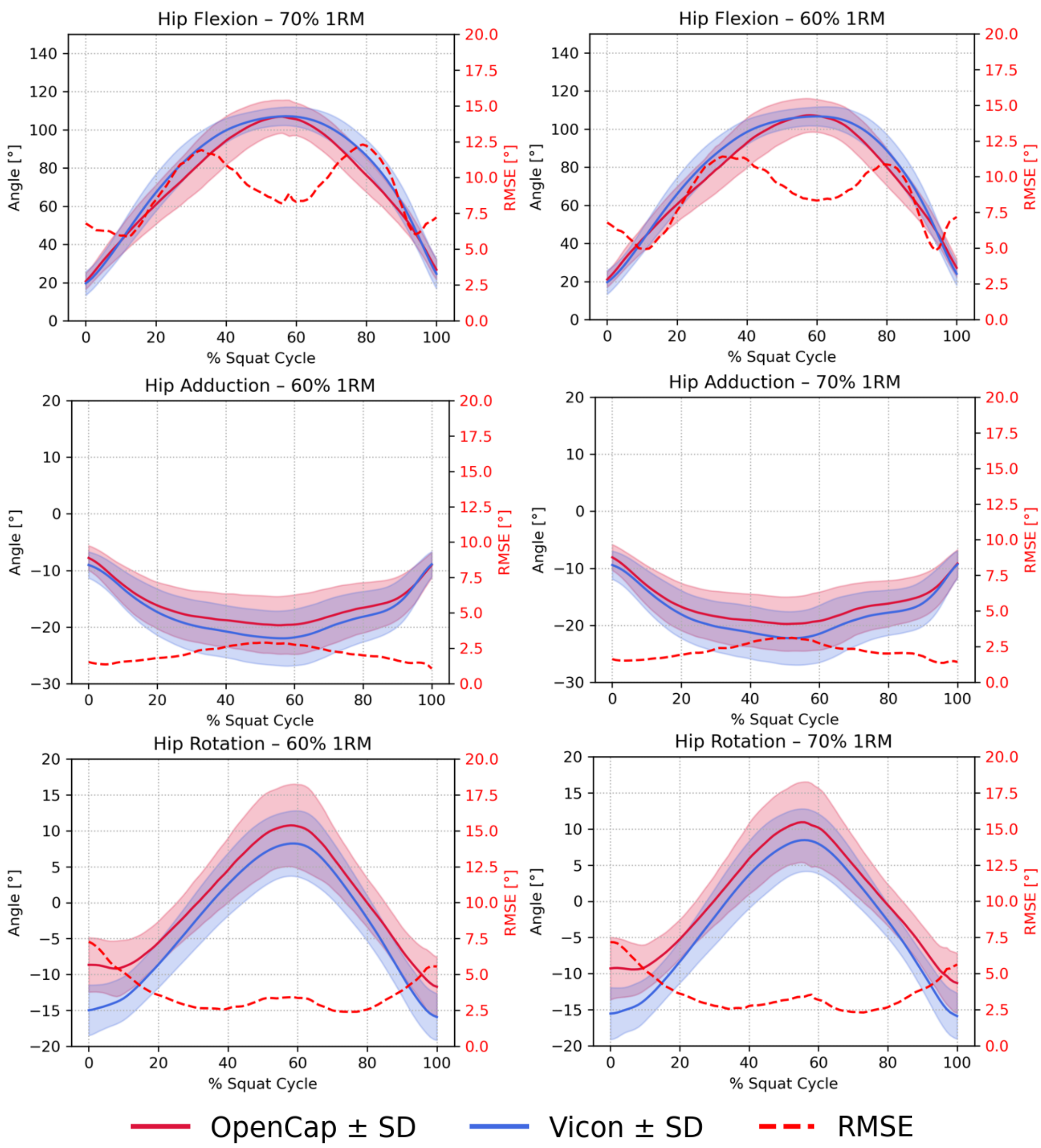

Figure 11: *Waveform-plots displaying the hip joint kinematics for the deep squat recorded with the markerless (red) and marker-based (blue) motion capture systems. The secondary axis shows the RMSE (red dashed) calculated per frame over the waveform of the squat cycle between both systems Plots are presented separately for both loading conditions.*

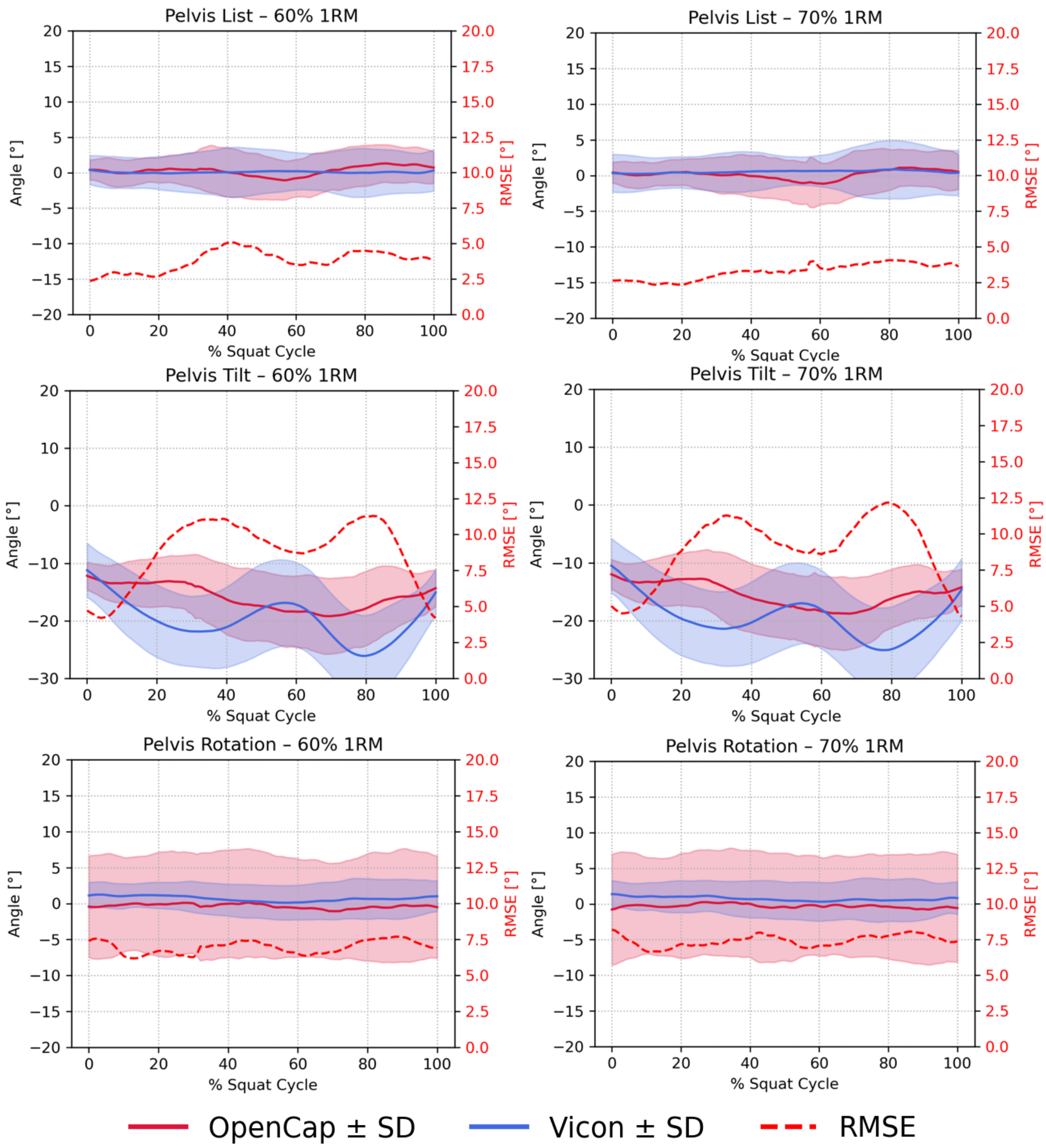

Figure 12: *Waveform-plots displaying the pelvis segment kinematics for the deep squat recorded with the markerless (red) and marker-based (blue) motion capture systems. The secondary axis shows the RMSE (red dashed) calculated per frame over the waveform of the squat cycle between both systems. Plots are presented separately for both loading conditions.*

5. Discussion

5.1 Evaluation of load-dependent changes

This study compared a markerless motion-capture system (OpenCap) and a marker-based system (Vicon) for assessing lower-body joint kinematics during barbell squats under varying loading conditions. SPM analysis revealed significant differences in kinematic variables between the 60% 1RM and 70% 1RM loading conditions for hip flexion, hip adduction, and knee flexion, whereas no significant effects were observed for pelvic variables, hip rotation, ankle flexion, and subtalar angle in the data of the marker-based system. This indicates a change in movement pattern with increasing load primarily affecting sagittal-plane hip and knee motion, as well as frontal-plane hip kinematics. These results align with previous studies that have evaluated changes in kinematic patterns under varying external loads during the barbell squat (Larsen et al., 2022). SPM analysis of the markerless data revealed an additional small, significant cluster in the subtalar angle, which may be due to large error values in that measure, indicating an impaired ability to accurately analyze kinematic changes in the subtalar angle. Furthermore, the markerless system detected only one significant cluster in hip flexion, indicating difficulty in tracking kinematic changes in hip flexion. For hip adduction and knee flexion, SPM analysis revealed the same clusters in markerless-system data as in marker-based data, indicating a strong ability to identify load-dependent kinematic changes in these variables.

Compared with these results, statistical analysis of differences in RMSE and mean bias between the two loading conditions revealed a significant increase in mean bias for hip flexion at 70% 1RM. This indicates that the markerless system systematically underestimated the hip flexion to a greater extent under higher intensities. The literature suggests a more forward trunk lean with increasing loads, which could have influenced the landmark tracking of the markerless system due to greater occlusion of the hip landmarks. In contrast, RMSE values for hip flexion presented no significant difference in the mean, which indicates that the overall magnitude of error did not increase, but rather the error shifted systematically in a direction. For knee flexion and hip adduction, no significant differences in RMSE or mean bias were observed, despite these variables showing load-dependent differences in the SPM analysis, indicating that the markerless syste was able to detect these kinematic changes. However, the paired t-test for mean bias in knee flexion was close to statistical significance, showing a potential load-dependent effect that could become relevant in larger samples. Evaluation of the boxplots revealed substantial variability and wide interquartile ranges across both loading conditions, while individual subject trajectories showed considerable inter-individual differences, with changes varying in magnitude and direction. This indicates that while group mean differences were small or absent for most agreement metrics, the variability reduced the ability to detect condition-dependent effects. Therefore, the absence of significant differences for most variables should not be taken for granted across all participants.

Overall, these results indicate that the markerless system provides stable kinematic analysis across different loading conditions, with joint- and plane-specific differences. However, these results should be interpreted with caution, as they may not be applicable to everyone due to substantial interindividual variability.

5.2 Evaluation of the agreement between the two MoCap systems

The markerless system demonstrated moderate agreement with the marker-based system compared to the predefined clinical thresholds. Previous OpenCap validation studies have predominantly relied on correlation-based and error-based metrics, such as CMC, RMSE, and MAE, with Bland–Altman analysis seldom applied in this context. Consequently, this study offers a complementary perspective by quantifying systematic bias and limits of agreement between the markerless and the marker-based reference. Although the mean bias between the markerless and the marker-based system was small, the wide limits of agreement indicate substantial variability across measurements. As these limits surpassed the predefined acceptable error threshold, the two systems cannot be considered interchangeable for precise joint-level kinematic assessment in this context. Our analysis showed an overall bias of 1.89° for the 60% 1 RM condition and an overall RMSE of 5.58°, with a peak error of 10.44°. For the 70%1RM condition, our analysis showed an overall bias of 1.71°, an overall RMSE of 5.61°, and a peak error of 10.43°. Therefore, the hypothesis that markerless and marker-based systems would demonstrate acceptable agreement within predefined error thresholds was not supported. These findings align with previous studies examining similar sport-specific movements (Lima et al., 2024; Yeom et al., 2026; Gow, 2023; Svetek et al., 2025). For instance, Yeom et al. (2026) reported an overall RMSE of 5.45° in the overhead squat, while Lima et al. (2024) observed a mean RMSE of 7.00° for the single-leg squat. Because the studies by Lima et al. (2024), Yeom et al. (2026), and Svetek et al. (2025) investigated movement tasks most comparable to those in the present study, they were used as primary references to contextualise our findings. To enable comparison with clinically oriented movement assessments, the study by Horsak et al. (2023) was also considered. Several plane- and joint-specific differences were identified in the Bland–Altman analysis and RMSE, which are discussed below, organised by movement plane and pelvis-segment kinematics.

5.2.1 Sagittal Plane

The sagittal plane analysis revealed that knee flexion showed the highest agreement, with a mean bias of 1.31° and an RMSE of 4.78° for the 60% 1RM condition, while the 70%1RM condition revealed a mean bias of 0.71 and a RMSE of 4.71. This RMSE is slightly lower than that reported by Lima et al. (2024) (5.3°) for the single-leg squat. In contrast, Svetek et al. (2025) found notably higher RMSE (approximately 8.00°) and mean bias (approximately 7°) for knee flexion during the body-weight squat. Such discrepancies may be attributable to the lower sampling rate of 60 Hz, the increased camera-subject distance of 5 m, and the presence of a safety bar that occluded the cameras' view in that study (Boey et al., 2025; Svetek et al., 2025). Although our knee flexion RMSE values were consistent with those reported by Lima et al. (2024), we observed lower errors for hip and ankle flexion. This improvement may be due to differences in the markerless motion capture setups; specifically, our study employed three cameras rather than two, which may have enhanced the accuracy of hip and ankle joint localisation. Previous research has indicated that 3D markerless accuracy improves with additional calibrated camera views (Varcin & Boocock, 2026), although Uhlrich et al. (2022) found no gains in accuracy with more cameras, suggesting the need for further investigation. Another possible reason for the higher RMSE in the single-leg squat is that participants in Lima et al. (2024) were instructed to place their hands on their hips, which may have obscured hip landmarks. The study by Yeom et al. (2026) reported a similar RMSE for hip flexion to that in the present study, possibly because the overhead squat is more comparable to the barbell back squat. Compared with non-sport-specific movements such as walking, our results indicate greater errors in hip and ankle flexion. For instance, Horsak et al. reported an RMSE of 5.4° for hip flexion and 4.6° for ankle flexion in physiological gait, whereas our findings indicate an RMSE of 8.31° (60% 1RM) and 8.62° (70% 1RM) for hip flexion and 7.95° (60% 1RM) and 7.75° (70% 1RM) for ankle flexion, both notably higher. These results highlight the challenge that markerless motion capture faces in capturing complex sports movements. One possible explanation is the large range of motion (ROM) in the squat; as a result, cameras may lose sight of pelvis segment landmarks at the lowest squat depth, affecting hip flexion measurement accuracy. Regarding the ankle ROM, the complexity of the foot segment may contribute to differences, with the marker set used for marker-based motion capture potentially yielding more accurate ankle angles.

5.2.2 Frontal Plane

In contrast to previous studies that reported limited agreement in the frontal plane, our results show good concordance between the markerless and the marker-based system for hip adduction, with a mean bias of 1.47° to 1.60° and an RMSE of 1.99° to 2.03° (Horsak et al., 2023; Lima et al., 2024; Svetek et al., 2025). This finding is further supported by a Bland–Altman analysis by Svetek et al. (2025), which documented a mean bias of 3.48° in hip movement in the frontal plane during the double-leg squat, with limits of agreement ranging from –8.33° to 10.47 °. The improved agreement in our study may be attributed to our camera setup, which used three perspectives, one directly visualizing the frontal plane, to enhance the accuracy of frontal plane movement reconstruction (Varcin & Boocock, 2026).

5.2.3 Transversal plane

A similar pattern is observed in the transverse plane for hip rotation. In this study, the RMSE for hip rotation ranged from 3.60° to 3.58°, with a peak error of 7.84° to 8.16. By comparison, other studies reported slightly higher errors, ranging from approximately 4.4° to 5.8° during related tasks (Liam et al., 2024; Yeom et al., 2026; Gow, 2023). These differences may again be attributable to variations in camera setup and the consistent movement pattern of the squat. Horsak et al. (2023) reported even higher RMSE values for hip rotation across various physiological and pathological gait patterns, from 6.6° to 8.4°, possibly indicating that the fixed stance width and continuous ground contact in the squat may improve measurement accuracy. In contrast to hip rotation, errors in the subtalar angle were consistent with previous studies (Horsak et al., 2023; Liam et al., 2024), reaffirming the complexity of the ankle joint reported in the literature for both marker-based and markerless systems.

5.2.4 Pelvis Segment

While the frontal and sagittal planes yielded promising results for the hip joint, analysis of the pelvis segment indicated low agreement between the markerless and the marker-based system. This finding is consistent with other studies assessing markerless system accuracy and is reflected in the higher RMSE values for pelvis tilt, list, and rotation observed in our study (Horsak et al., 2023; Liam et al., 2024). One likely explanation is that the femur obscures the pelvis during the lowest phase of the squat, which impairs the markerless system's ability to track body landmarks accurately. This limitation may also affect the marker-based system. Notably, to address this issue, our protocol included four additional pelvic markers and employed gap-filling algorithms to reconstruct missing front pelvic markers when they were not visible. The implications of these results will be further explored in the subsequent discussion.

5.3 Application of the markerless system OpenCap

The applicability of the markerless system for analyzing the barbell squat depends largely on the intended purpose, which may include performance and technique analysis, injury prevention, or rehabilitation. Some kinematic variables demonstrate sufficient agreement to support exploratory or descriptive use. However, other variables have limitations that constrain the system's suitability for diagnostic or clinical applications. The following section synthesizes these perspectives to provide a comprehensive assessment of the markerless system's practical utility.

Kinematic analysis of the squat is fundamental for identifying movement-related errors, particularly from a performance and technique perspective. This is especially relevant in the sticking region, where barbell velocity decreases and the risk of failure peaks during the concentric phase (Kristiansen et al., 2021). Analysis of joint angles helps sports scientists determine whether failure results from unfavorable biomechanical leverage (Kristiansen et al., 2021; Larsen et al., 2021). Previous research indicates that an unfavorable position of the hip extensors contributes to this velocity loss (Larsen et al., 2021; Larsen et al., 2025), underscoring the importance of assessing hip flexion and extension when diagnosing technique-related performance limitations.

Our results indicate poor agreement between the markerless and the marker-based system for hip extension and flexion. The bias indicates that the markerless system consistently underestimates the hip flexion angle by -3.33° to -4.23°, with an RMSE of 8.31° to 8.62° and a peak error of 15.37° to 15.67°. Additionally, the limits of agreement (LoA) are broad, ranging from ≈ -20.00° to ≈12.50°. Given these findings, the markerless system cannot yet provide precise information about the primary cause of the sticking region in the barbell squat. Based on the categorization of agreement in the literature, the markerless system should be used cautiously when identifying technical errors in high-performance athletes. This limitation is notable because the sticking region occurs during the concentric phase (Kristiansen et al., 2017). Consistent with this, the RMSE waveform (Figure 11) shows increased errors during both the concentric and eccentric phases of the squat.

Performance analysis often extends beyond identifying isolated technique errors to include comparisons of squat variations across kinematic and kinetic variables (Pürzel et al., 2025; Glassbrook et al., 2019). Lower-body kinematics are known to differ between squatting variations, such as the LowBar squat (LBS) and the HighBar squat (HBS). Significant differences in the hip joint are observed across the frontal and sagittal planes, with standing width strongly affecting hip abduction and rotation (Larsen et al., 2021). Hip abduction and rotation are typically about 7° higher in the LBS compared to the HBS (Larsen et al., 2021; Larsen et al., 2024). Our findings indicate good agreement for these kinematic variables, with biases ranging from 2.96° to 2.98° for hip rotation and from 1.47° to 1.60° for hip adduction, and RMSEs of 3.60° to 3.58° for hip rotation and 1.99° to 2.03° for hip adduction. Because these errors are smaller than the observed differences between squat variations, the markerless system may detect kinematic changes in the hip in the frontal and sagittal planes. However, when comparing the two variations, researchers have also observed differences in hip, knee, and ankle flexion. LBS results in approximately 5° greater hip flexion (Kristiansen et al., 2021; Larsen et al., 2021; Larsen et al., 2024). As previously noted, the markerless system shows poor agreement for hip flexion and yields an RMSE higher than the expected change in hip flexion across squat variations, limiting its ability to detect precise technique changes. The same limitation applies to ankle flexion, which is influenced by standing width; a narrow stance produces approximately 10° greater ankle flexion (Larsen et al., 2021; Kristiansen et al., 2021) The RMSE for ankle flexion in our study ranges from 7.95° to 7.75°, depending on the condition, which is close to the magnitude of the technique-related change.

For knee flexion, the markerbased system tends to overestimate the angle by ≈1°, indicating good agreement. Squatting technique changes can result in up to 10° changes in knee flexion. The markerless system may be able to identify these changes. Therefore, the markerless system could be useful for detecting changes in squatting variations when marker-based systems are unavailable. Nonetheless, caution is required when analyzing differences in hip and ankle flexion.

Performance-related limitations of the markerless system also have significant implications for injury prevention. Accurate assessment of knee alignment, ankle joint mobility, and pelvic tilt is crucial during the barbell squat. For example, biomechanical analysis is necessary to diagnose medial knee displacement (knee valgus), which elevates anterior cruciate ligament (ACL) strain (Schönfeld, 2010). Because the markerless system cannot track knee movement in the frontal plane, it cannot be used to identify potential valgus issues.

Pelvic tilt is a key factor during the squat, as it helps minimize shear forces on the lumbar spine and reduce the risk of intervertebral disc injury (Schönfeld, 2010; Kristiansen et al., 2021). Our results show poor accuracy in pelvic tilt analysis. The markerless system consistently overestimates pelvic tilt by approximately 4°, with limits of agreement (LoA) ranging from ≈ -12.00° to ≈ 20.00°. The RMSE is also high at ≈ 8.40°. Given the limited range of motion observed in the waveforms in Figure 12, these errors account for a large percentage of the total movement, compromising the ability to accurately analyze pelvic tilt. Ankle mobility is another important factor in injury prevention during the barbell squat. Stabilizing the body during movement and maintaining full-foot contact with the floor are essential (Schönfeld, 2010; Van den Tillar & Larsen, 2020). Our results align with previous studies and indicate poor validity in the analysis of ankle flexion and the subtalar angle. The markerless system tends to overestimate ankle flexion by approximately 7°, indicating poor agreement.

Due to the inability to analyze the frontal plane of the knee joint and the poor agreement for pelvic tilt, ankle flexion, and the subtalar angle, we recommend caution when using the markerless system as a diagnostic tool for injury prevention and joint safety analysis in the barbell squat.

These limitations also apply to rehabilitation settings, where squat analysis is commonly used to evaluate movement safety in individuals with patellar tendinopathy or after anterior cruciate ligament rupture (Scattone Silva et al., 2024). Knee joint alignment is particularly important (Schönfeld, 2010). Since knee alignment is heavily influenced by hip and pelvic kinematics, these variables are essential for assessing squat safety during rehabilitation. Because the markerless system showed poor agreement for these variables and cannot analyze the frontal plane of the knee joint, its use as a markerless system in rehabilitation should be recommended with caution.

5.4 Limitations

Several limitations should be considered when interpreting the findings of this study. The participant group consisted mainly of healthy, physically active sports students, which may limit generalizability to other populations such as older individuals or elite powerlifters. Nevertheless, the results remain relevant for recreationally trained athletes performing barbell squats under controlled conditions, a population commonly targeted in performance analysis and clinical screening.

All squats were performed without additional equipment and with minimal clothing. In applied settings, athletes often wear knee sleeves, lifting belts, or squat-specific footwear, which may affect the visibility of anatomical landmarks and the accuracy of markerless motion capture. The standardized clothing conditions in this study reduced potential confounding effects and are appropriate for a validation setting, consistent with previous findings reporting only minor clothing-related errors (Horsak et al., 2023).

The analysis was limited to moderate squat intensities. At higher loads, smaller compensatory movements may lead to greater kinematic discrepancies. However, the absence of accuracy differences between the tested loading conditions suggests that the markerless system's performance is not substantially affected by moderate increases in intensity, supporting its applicability within this range.

5.5 Future Research

Our analysis demonstrated moderate to good agreement between the markerless and the mrker-based system, depending on the joint and plane of movement. These findings suggest that the mrkerless system has potential for future applications, although its performance is not yet optimal. The markerless system's pose estimation algorithm uses OpenPose to extract two-dimensional (2D) keypoints and triangulate them to compute three-dimensional (3D) poses. In addition, a recurrent neural network is employed to transform the 2D keypoints into a 3D anatomical marker set. OpenPose is primarily trained on the COCO dataset, which primarily comprises everyday and situational movements rather than sport-specific movements such as the squat (Uhlrich et al., 2022). Our results indicate that this training approach may be insufficient to accurately estimate kinematics for movements outside everyday activities. This limitation has also been reported for pathological gait patterns by Horsak et al. (2023). It is possible that accuracy in pose estimation for sport-specific tasks could be improved by training both the OpenPose algorithm and the markerless system's recurrent neural network with sport-specific data.

The bias and RMSE for pelvic tilt, list, rotation, and hip flexion were notably higher than values reported in other studies analyzing different movement patterns (Horsak et al., 2023; Liam et al., 2024; Yeom et al., 2025). This discrepancy may be attributed to the large range of motion (ROM) during the squat, which decreases the visibility of the hip and pelvis segments at the lowest squat position. Addressing this issue could involve enabling the markerless system to record in a 360° field of view around the participant, thereby ensuring that body landmarks remain visible in at least two cameras at most times. Additionally, adjustments to the marker set — such as those implemented in our marker-based setup by adding four additional markers to the pelvis segment — could improve reconstruction of the frontal pelvic markers when these landmarks are not visible. These technical enhancements may support more accurate data collection in future applications.

Analysis of the RMSE waveform presented in Figure 9-12 shows that RMSE values are higher during the concentric and eccentric phases of the squat for variables in the sagittal plane. This outcome may result from the lower 120 Hz frame rate used for the markerless system during data collection. Although the markerless system can record at 240 Hz, this setting is limited to 15 seconds, which was inadequate to capture the entire trial in our analysis. Comprehensive data collection required recording the walk-out and walk-in to ensure reliability. Extending recording time at higher frame rates may enhance accuracy during the dynamic phases of the squat. These considerations underscore the importance of technical parameters in obtaining precise kinematic measurements.

During data collection, the model reached its anatomical limits for knee, hip, or ankle flexion in 35 trials, indicating that participants could achieve joint angles beyond those permitted by the model. Specifically, the underlying model restricts flexion to 140° for the knee, 120° for the hip, and 50° for the ankle. Consequently, the LaiUhlrich2022 model may not be optimal for analyzing the squat in elite powerlifters, as the literature suggests that knee, ankle, and hip flexion in this population may exceed these thresholds. Adjusting the anatomical limits within the model may improve the accuracy and relevance of squat analysis in such populations. This limitation highlights the importance of model selection and customization for sport-specific biomechanics research.

Although tracking joint kinematics alone may not provide a comprehensive analysis of the squat, the markerless system also offers estimation algorithms for kinetic data, including joint moments and ground reaction forces. Further research should evaluate the accuracy of these algorithms, as such data are critical for assessing technical aspects of the squat in performance athletes, as well as for health prevention and rehabilitation. Validation of the markerless system in a variety of sport-specific tasks remains essential for future studies. It should be noted that our findings reflect the accuracy of the markerless system exclusively within a controlled laboratory environment. Future investigations should assess the performance of kinematic analysis in real-world scenarios, such as training sessions and competitions. Moreover, exploring the markerless system with a musculoskeletal model tailored for squats and featuring increased anatomical limits could provide additional insights. Additional directions for future research should investigate whether increasing the number of cameras and frame rate improves the markerless system's ability to record sufficient kinematic data. These future directions will contribute to a more robust evaluation of the markerless system's utility in sports biomechanics.

6. Conclusion

In summary, the markerless system provides a simple and easy-to-use biomechanics analysis tool. It shows moderate performance in estimating joint kinematics relative to predefined thresholds. However, our findings suggest a lack of joint- and plane-specific agreement, and caution should be exercised when using markerless MoCap for clinical, scientific, and performance-related purposes. Limited training data on sport-specific movements may contribute to discrepancies. Markerless motion capture holds great promise for biomechanical research beyond laboratory settings. Continuous algorithmic training has the potential to enhance its accuracy. Markerless MoCap has the potential to become widely accessible, which could benefit educational purposes in sport-related studies. Lecturers could teach students the basics of biomechanical analysis using markerless motion capture systems, since marker-based systems are not always available and are more time-consuming. We anticipate continued advances in markerless systems and the promising benefits they offer for motion analysis.

Literature

1. Adlou, B., Wilburn, C., & Weimar, W. (2025). Motion Capture Technologies for Athletic Performance Enhancement and Injury Risk Assessment: A Review for Multi-Sport Organizations. *Sensors (Basel, Switzerland)*, *25*(14), 4384. https://doi.org/10.3390/s25144384
2. Armitano-Lago, C., Willoughby, D., & Kiefer, A. W. (2022). A SWOT Analysis of Portable and Low-Cost Markerless Motion Capture Systems to Assess Lower-Limb Musculoskeletal Kinematics in Sport. *Frontiers in sports and active living*, *3*, 809898. https://doi.org/10.3389/fspor.2021.809898
3. Bland, J. M., & Altman, D. G. (1999). Measuring agreement in method comparison studies. *Statistical Methods in Medical Research,* *8*(2), 135–160. https://doi.org/10.1177/096228029900800204
4. Boey, D., Girard, O., Lee, M., Elliott, B., & Reid, M. (2025). Unlocking the potential of video-based markerless motion analysis to study world-class sporting performance. *Journal of sports sciences*, 1–14. Advance online publication. https://doi.org/10.1080/02640414.2025.2576412
5. Bryanton, M. A., Kennedy, M. D., Carey, J. P., & Chiu, L. Z. (2012). Effect of squat depth and barbell load on relative muscular effort in squatting. *Journal of strength and conditioning research*, *26*(10), 2820–2828. https://doi.org/10.1519/JSC.0b013e31826791a7
6. Ceseracciu, E., Sawacha, Z., & Cobelli, C. (2014). Comparison of markerless and marker-based motion capture technologies through simultaneous data collection during gait: proof of concept. *PloS one*, *9*(3), e87640. https://doi.org/10.1371/journal.pone.0087640
7. Chaumeil, A., Lahkar, B. K., Dumas, R., Muller, A., & Robert, T. (2024). Agreement between a markerless and a marker-based motion capture systems for balance related quantities. *Journal of biomechanics*, *165*, 112018. https://doi.org/10.1016/j.jbiomech.2024.112018
8. Das, K., de Paula Oliveira, T., & Newell, J. (2023). Comparison of markerless and marker-based motion capture systems using 95% functional limits of agreement in a linear mixed-effects modelling framework. *Scientific Reports, 13*, Article 22880. https://doi.org/10.1038/s41598-023-49360-2
9. Delp, S. L., Anderson, F. C., Arnold, A. S., Loan, P., Habib, A., John, C. T., Guendelman, E., & Thelen, D. G. (2007). OpenSim: open-source software to create and analyze dynamic simulations of movement. *IEEE transactions on bio-medical engineering*, *54*(11), 1940–1950. https://doi.org/10.1109/TBME.2007.901024
10. Escamilla, R. F., Fleisig, G. S., Lowry, T. M., Barrentine, S. W., & Andrews, J. R. (2001). A three-dimensional biomechanical analysis of the squat during varying stance widths. *Medicine and science in sports and exercise*, *33*(6), 984–998. https://doi.org/10.1097/00005768-200106000-00019
11. Falisse, A., Uhlrich, S. D., Chaudhari, A. S., Hicks, J. L., & Delp, S. L. (2025). Marker Data Enhancement for Markerless Motion Capture. *IEEE transactions on bio-medical engineering*, *72*(6), 2013–2022. https://doi.org/10.1109/TBME.2025.3530848
12. Giustino, V., & Patti, A. (2025). Biomechanics and Sports Performances. *Sports (Basel, Switzerland)*, *13*(3), 73. https://doi.org/10.3390/sports13030073
13. Glassbrook, D. J., Brown, S. R., Helms, E. R., Duncan, S., & Storey, A. G. (2019). The High-Bar and Low-Bar Back-Squats: A Biomechanical Analysis. *Journal of strength and conditioning research*, *33 Suppl 1*, S1–S18. https://doi.org/10.1519/JSC.0000000000001836
14. Goodman, W., Flores, V., Cotter, J. A., Graham, D., & Becker, J. (2024). Support moment distribution during the back squat at different depths and loads in recreationally trained females. *Journal of science and medicine in sport*, *27*(2), 119–124. https://doi.org/10.1016/j.jsams.2023.11.001
15. Gow, R. (2023). *Evaluation of a smartphone-based motion capture system for athletic movement screening* (Master's thesis, University of California, San Diego). University of California eScholarship.

16. Haff, G. G., & Triplett, N. T. (Eds.). (2015). *Essentials of strength training and conditioning* (4th ed.). Human Kinetics.
17. Hammami, M., Gaamouri, N., Shephard, R. J., & Chelly, M. S. (2019). Effects of Contrast Strength vs. Plyometric Training on Lower-Limb Explosive Performance, Ability to Change Direction and Neuromuscular Adaptation in Soccer Players. *Journal of strength and conditioning research*, *33*(8), 2094–2103. https://doi.org/10.1519/JSC.0000000000002425
18. Höltke, T., Vegter, R. J. K., Brink, M. S., & Janssen, I. (2025). Lower limb movement asymmetry exists during volleyball stop-jump landing: Insights from markerless motion capture. *Journal of sports sciences*, 1–11. Advance online publication. https://doi.org/10.1080/02640414.2025.2490883
19. Horsak, B., Eichmann, A., Lauer, K., Prock, K., Krondorfer, P., Siragy, T., & Dumphart, B. (2023). Concurrent validity of smartphone-based markerless motion capturing to quantify lower-limb joint kinematics in healthy and pathological gait. *Journal of biomechanics*, *159*, 111801. https://doi.org/10.1016/j.jbiomech.2023.111801
20. Jatesiktat, P., Lim, G. M., Lim, W. S., & Ang, W. T. (2025). Anatomical-Marker-Driven 3D Markerless Human Motion Capture. *IEEE journal of biomedical and health informatics*, *29*(9), 6186–6199. https://doi.org/10.1109/JBHI.2024.3424869
21. Kanko, R. M., Laende, E. K., Davis, E. M., Selbie, W. S., & Deluzio, K. J. (2021). Concurrent assessment of gait kinematics using marker-based and markerless motion capture. *Journal of biomechanics*, *127*, 110665. https://doi.org/10.1016/j.jbiomech.2021.110665
22. Kristiansen, E., Larsen, S., Haugen, M. E., Helms, E., & van den Tillaar, R. (2021). A Biomechanical Comparison of the Safety-Bar, High-Bar and Low-Bar Squat around the Sticking Region among Recreationally Resistance-Trained Men and Women. *International journal of environmental research and public health*, *18*(16), 8351. https://doi.org/10.3390/ijerph18168351
23. Lai, A.K., Arnold, A.S., Wakeling, J.M., 2017. Why are antagonist muscles co-activated in my simulation? A musculoskeletal model for analysing human locomotor tasks. Ann. Biome
24. Lam, W. W. T., Tang, Y. M., & Fong, K. N. K. (2023). A systematic review of the applications of markerless motion capture (MMC) technology for clinical measurement in rehabilitation. *Journal of neuroengineering and rehabilitation*, *20*(1), 57. https://doi.org/10.1186/s12984-023-01186-9
25. Larsen, S., de Zee, M., Kristiansen, E. L., & van den Tillaar, R. (2024). A Biomechanical Comparison Between a High and Low Barbell Placement on Net Joint Moments, Kinematics, Muscle Forces, and Muscle-Specific Moments in 3 Repetition Maximum Back Squats. *Journal of strength and conditioning research*, *38*(7), 1221–1230. https://doi.org/10.1519/JSC.0000000000004790
26. Larsen, S., Kristiansen, E., & van den Tillaar, R. (2021). New Insights About the Sticking Region in Back Squats: An Analysis of Kinematics, Kinetics, and Myoelectric Activity. *Frontiers in sports and active living*, *3*, 691459. https://doi.org/10.3389/fspor.2021.691459
27. Larsen, S., Kristiansen, E., Helms, E., & van den Tillaar, R. (2021). Effects of Stance Width and Barbell Placement on Kinematics, Kinetics, and Myoelectric Activity in Back Squats. *Frontiers in sports and active living*, *3*, 719013. https://doi.org/10.3389/fspor.2021.719013
28. Larsen, S., Kristiansen, E., Nygaard Falch, H., Estifanos Haugen, M., Fimland, M. S., & van den Tillaar, R. (2025). Effects of barbell load on kinematics, kinetics, and myoelectric activity in back squats. *Sports biomechanics*, *24*(10), 2856–2870. https://doi.org/10.1080/14763141.2022.2085164
29. Larsen, S., Kristiansen, E., Nygaard Falch, H., Estifanos Haugen, M., Fimland, M. S., & van den Tillaar, R. (2025). Effects of barbell load on kinematics, kinetics, and myoelectric activity in back squats. *Sports biomechanics*, *24*(10), 2856–2870. https://doi.org/10.1080/14763141.2022.2085164
30. Larsen, S., Zee, M., & Tillaar, R. V. D. (2025). The Impact of Stance Width on Kinematics and Kinetics During Maximum Back Squats. *Journal of strength and conditioning research*, *39*(1), 1–9. https://doi.org/10.1519/JSC.0000000000004949

31. Leboeuf, F., Baker, R., Barré, A., Reay, J., Jones, R., & Sangeux, M. (2019). The conventional gait model, an open-source implementation that reproduces the past but prepares for the future. *Gait & posture*, *69*, 235–241. https://doi.org/10.1016/j.gaitpost.2019.04.015
32. Liao, Y., Vakanski, A., Xian, M., Paul, D., & Baker, R. (2020). A review of computational approaches for evaluation of rehabilitation exercises. *Computers in biology and medicine*, *119*, 103687. https://doi.org/10.1016/j.compbiomed.2020.103687
33. Lima, Y. L., Collings, T., Hall, M., Bourne, M. N., & Diamond, L. E. (2024). Validity and reliability of trunk and lower-limb kinematics during squatting, hopping, jumping and side-stepping using OpenCap markerless motion capture application. *Journal of sports sciences*, *42*(19), 1847–1858. https://doi.org/10.1080/02640414.2024.2415233
34. Loturco, I., Pereira, L. A., Reis, V. P., Zanetti, V., Bishop, C., & McGuigan, M. R. (2022). Traditional Free-Weight Vs. Variable Resistance Training Applied to Elite Young Soccer Players During a Short Preseason: Effects on Strength, Speed, and Power Performance. *Journal of strength and conditioning research*, *36*(12), 3432–3439. https://doi.org/10.1519/JSC.0000000000003899
35. Matsuda, T., Fujino, Y., Morisawa, T., Takahashi, T., Kakegawa, K., Matsumoto, T., Kiyohara, T., Fukushima, H., Higuchi, M., Torimoto, Y., Miwa, M., Fujiwara, T., & Daida, H. (2025). Reliability and Validity Examination of a New Gait Motion Analysis System. *Sensors (Basel, Switzerland)*, *25*(4), 1076. https://doi.org/10.3390/s25041076
36. Mündermann, L., Corazza, S., & Andriacchi, T. P. (2006). The evolution of methods for the capture of human movement leading to markerless motion capture for biomechanical applications. *Journal of neuroengineering and rehabilitation*, *3*, 6. https://doi.org/10.1186/1743-0003-3-6
37. McGinley, J. L., Baker, R., Wolfe, R., & Morris, M. E. (2009). The reliability of three-dimensional kinematic gait measurements: a systematic review. *Gait & posture*, *29*(3), 360–369. https://doi.org/10.1016/j.gaitpost.2008.09.003
38. Murawa, M., Fryzowicz, A., Kabacinski, J., Jurga, J., Gorwa, J., Galli, M., & Zago, M. (2020). Muscle activation varies between high-bar and low-bar back squat. *PeerJ*, *8*, e9256. https://doi.org/10.7717/peerj.9256
39. Myer, G. D., Kushner, A. M., Brent, J. L., Schoenfeld, B. J., Hugentobler, J., Lloyd, R. S., Vermeil, A., Chu, D. A., Harbin, J., & McGill, S. M. (2014). The back squat: A proposed assessment of functional deficits and technical factors that limit performance. *Strength and conditioning journal*, *36*(6), 4–27. https://doi.org/10.1519/SSC.0000000000000103
40. Pallarés, J. G., Cava, A. M., Courel-Ibáñez, J., González-Badillo, J. J., & Morán-Navarro, R. (2020). Full squat produces greater neuromuscular and functional adaptations and lower pain than partial squats after prolonged resistance training. *European journal of sport science*, *20*(1), 115–124. https://doi.org/10.1080/17461391.2019.1612952
41. Pataky T. C. (2012). One-dimensional statistical parametric mapping in Python. *Computer methods in biomechanics and biomedical engineering*, *15*(3), 295–301. https://doi.org/10.1080/10255842.2010.527837
42. Pürzel, A., Kaufmann, P., Koller, W., Pöhlmann, L., Baca, A., & Kainz, H. (2025). Muscle Force Dynamics Across Increasing Squat Intensity Conditions in Elite Powerlifters. *Scandinavian journal of medicine & science in sports*, *35*(5), e70058. https://doi.org/10.1111/sms.70058
43. Pürzel, A., Kaufmann, P., Koller, W., Wallnöfer, E. K., Baca, A., & Kainz, H. (2025). Biomechanical analysis of hip, knee, and ankle joint contact forces during squats in elite powerlifters. *PloS one*, *20*(7), e0327973. https://doi.org/10.1371/journal.pone.0327973
44. Rajagopal, A., Dembia, C.L., DeMers, M.S., Delp, D.D., Hicks, J.L., Delp, S.L., 2016. Full-body musculoskeletal model for muscle-driven simulation of human gait. IEEE Trans. Bio-Med. Eng. 6
45. Ray, L. S. S., Zhou, B., Suh, S., & Lukowicz, P. (2024). A comprehensive evaluation of marker-based, markerless methods for loose garment scenarios in varying camera configurations**.** *Frontiers in Computer Science,* *6*, Article 1379925. https://doi.org/10.3389/fcomp.2024.1379925
46. Rojas-Jaramillo, A., Cuervo-Arango, D. A., Quintero, J. D., Ascuntar-Viteri, J. D., Acosta-Arroyave, N., Ribas-Serna, J., González-Badillo, J. J., & Rodríguez-Rosell, D. (2024). Impact of

the deep squat on articular knee joint structures, friend or enemy? A scoping review. *Frontiers in sports and active living*, *6*, 1477796. https://doi.org/10.3389/fspor.2024.1477796
47. Scataglini, S., Abts, E., Van Bocxlaer, C., Van den Bussche, M., Meletani, S., & Truijen, S. (2024). Accuracy, Validity, and Reliability of Markerless Camera-Based 3D Motion Capture Systems versus Marker-Based 3D Motion Capture Systems in Gait Analysis: A Systematic Review and Meta-Analysis. *Sensors (Basel, Switzerland)*, *24*(11), 3686. https://doi.org/10.3390/s24113686
48. Scattone Silva, R., Song, K. E., Hullfish, T. J., Sprague, A., Silbernagel, K. G., & Baxter, J. R. (2024). Patellar Tendon Load Progression during Rehabilitation Exercises: Implications for the Treatment of Patellar Tendon Injuries. *Medicine and science in sports and exercise*, *56*(3), 545–552. https://doi.org/10.1249/MSS.0000000000003323
49. Schoenfeld B. J. (2010). Squatting kinematics and kinetics and their application to exercise performance. *Journal of strength and conditioning research*, *24*(12), 3497–3506. https://doi.org/10.1519/JSC.0b013e3181bac2d7
50. Sohn, J., & Koo, D. (2023). Effects of load increase on lower extremity kinetic and kinematic variables in the back squat exercise. *Technology and health care : official journal of the European Society for Engineering and Medicine*, *31*(S1), 247–258. https://doi.org/10.3233/THC-236021
51. Souaifi, M., Dhahbi, W., Jebabli, N., Ceylan, H. İ., Boujabli, M., Muntean, R. I., & Dergaa, I. (2025). Artificial Intelligence in Sports Biomechanics: A Scoping Review on Wearable Technology, Motion Analysis, and Injury Prevention. *Bioengineering (Basel, Switzerland)*, *12*(8), 887. https://doi.org/10.3390/bioengineering12080887
52. Stone, M. H., Hornsby, G., Mizuguchi, S., Sato, K., Gahreman, D., Duca, M., Carroll, K., Ramsey, M. W., Stone, M. E., & Haff, G. G. (2024). The Use of Free Weight Squats in Sports: A Narrative Review-Squatting Movements, Adaptation, and Sports Performance: Physiological. *Journal of strength and conditioning research*, *38*(8), 1494–1508. https://doi.org/10.1519/JSC.0000000000004838
53. Straub, R. K., & Powers, C. M. (2024). A Biomechanical Review of the Squat Exercise: Implications for Clinical Practice. *International journal of sports physical therapy*, *19*(4), 490–501. https://doi.org/10.26603/001c.94600
54. Styles, W. J., Matthews, M. J., & Comfort, P. (2016). Effects of Strength Training on Squat and Sprint Performance in Soccer Players. *Journal of strength and conditioning research*, *30*(6), 1534–1539. https://doi.org/10.1519/JSC.0000000000001243
55. Suo, X., Tang, W., & Li, Z. (2024). Motion Capture Technology in Sports Scenarios: A Survey. *Sensors (Basel, Switzerland)*, *24*(9), 2947. https://doi.org/10.3390/s24092947
56. Tai, W. H., Zhang, R., & Zhao, L. (2023). Cutting-Edge Research in Sports Biomechanics: From Basic Science to Applied Technology. *Bioengineering (Basel, Switzerland)*, *10*(6), 668. https://doi.org/10.3390/bioengineering10060668
57. Teferi, G., & Endalew, D. (2020). Methods of Biomechanical Performance Analyses in Sport: Systematic Review. *American Journal of Sports Science and Medicine, 8*, 47-52.
58. Turner, J. A., Chaaban, C. R., & Padua, D. A. (2024). Validation of OpenCap: A low-cost markerless motion capture system for lower-extremity kinematics during return-to-sport tasks. *Journal of Biomechanics*, *171*, 112200. https://doi.org/10.1016/j.jbiomech.2024.112200
59. Uhlrich, S. D., Falisse, A., Kidziński, Ł., Muccini, J., Ko, M., Chaudhari, A. S., Hicks, J. L., & Delp, S. L. (2023). OpenCap: Human movement dynamics from smartphone videos. *PLoS computational biology*, *19*(10), e1011462. https://doi.org/10.1371/journal.pcbi.1011462
60. van den Tillaar, R., & Larsen, S. (2020). Kinematic and EMG Comparison Between Variations of Unilateral Squats Under Different Stabilities. *Sports medicine international open*, *4*(2), E59–E66. https://doi.org/10.1055/a-1195-1039
61. van den Tillaar, R., Falch, H. N., & Larsen, S. (2024). Are Diminishing Potentiation and Large Extensor Moments the Cause for the Occurrence of the Sticking Region in Maximum Free-Weight Barbell Back Squats among Resistance-Trained Males?. *Journal of human kinetics*, *91*(Spec Issue), 105–119. https://doi.org/10.5114/jhk/185720

62. van den Tillaar, R., Andersen, V., & Saeterbakken, A. H. (2019). Comparison of muscle activation and kinematics during free-weight back squats with different loads. *PloS one*, *14*(5), e0217044. https://doi.org/10.1371/journal.pone.0217044
63. van der Kruk, E., & Reijne, M. M. (2018). Accuracy of human motion capture systems for sport applications; state-of-the-art review. *European journal of sport science*, *18*(6), 806–819. https://doi.org/10.1080/17461391.2018.1463397
64. Varcin, F., & Boocock, M. G. (2026). The accuracy, validity and reliability of Theia3D markerless motion capture for studying the biomechanics of human movement: A systematic review. *Artificial intelligence in medicine*, *173*, 103332. https://doi.org/10.1016/j.artmed.2025.103332
65. Wade, L., Needham, L., McGuigan, P., & Bilzon, J. (2022). Applications and limitations of current markerless motion capture methods for clinical gait biomechanics. *PeerJ*, *10*, e12995. https://doi.org/10.7717/peerj.12995
66. Wei, L., Yang, C., Huang, X., Tu, L., Xu, Y., Li, M., & Hu, Z. (2025). Comparison of lower limb kinematics and kinetics estimation of basketball players during jumping with markerless and marker-based motion capture systems. *Acta of bioengineering and biomechanics*, *27*(2), 133–145. https://doi.org/10.37190/abb/207092
67. Winter, D. A. (2009). *Biomechanics and motor control of human movement* (4th ed.). John Wiley & Sons.
68. Wren, T. A. L., Isakov, P., & Rethlefsen, S. A. (2023). Comparison of kinematics between Theia markerless and conventional marker-based gait analysis in clinical patients. *Gait & posture*, *104*, 9–14. https://doi.org/10.1016/j.gaitpost.2023.05.029
69. Yang, H. S. (2024). Advances in markerless motion capture systems: A review of OpenCap and its applications. *The Asian Journal of Kinesiology,* *26*(4), 42–47. https://doi.org/10.15758/ajk.2024.26.4.42
70. Yeom, S., Jeong, B., Lee, J., Hyung, S. K., Kim, H., Chang, E., & Kim, K. M. (2026). Validation of Markerless Motion Capture System (OpenCap) for Overhead Squat Kinematics. *Measurement in Physical Education and Exercise Science*, *30*(1), 49–62. https://doi.org/10.1080/1091367X.2025.2512361

Eidesstattliche Erklärung

“Ich erkläre, dass ich die vorliegende Arbeit selbstständig verfasst habe und nur die ausgewiesenen Hilfsmittel verwendet habe. Diese Arbeit wurde weder an einer anderen Stelle eingereicht (z.B. für andere Lehrveranstaltungen) noch von anderen Personen (z.B. Arbeiten von anderen Personen aus dem Internet) vorgelegt.“